REVIEW PAPER

Hydrophobization of lignocellulosic materials part II: chemical modification

Sandra Rodríguez-Fabià [ID] ·
Jonathan Torstensen [ID] · **Lars Johansson** [ID] ·
Kristin Syverud [ID]

Abstract Lignocellulosic materials with hydrophobic properties are of great interest for developing sustainable products that can be used in various applications such as packaging, water-repellent and self-cleaning materials, oil and water separation or as reinforcements in biocomposite materials. The hydroxyl functional groups present in cellulose provide the possibility to perform various chemical modifications to the cellulosic substrates that can increase their hydrophobicity. This review is the second part of a comprehensive review on hydrophobization of lignocellulosic materials and summarizes the recent advances in the chemical modification of such substrates. The methods described in this review can provide changes in the hydrophilicity of the materials that range from a small decrease in the initial hydrophilicity of the substrate (contact angles below 90°) to superhydrophobic properties (contact angles above 150°). Additional attention has been paid to whether the modification is limited to the surface of the substrate or if it occurs in the bulk of the material. We also discuss hydrophobized cellulose material applications in packing and oil/water purification.
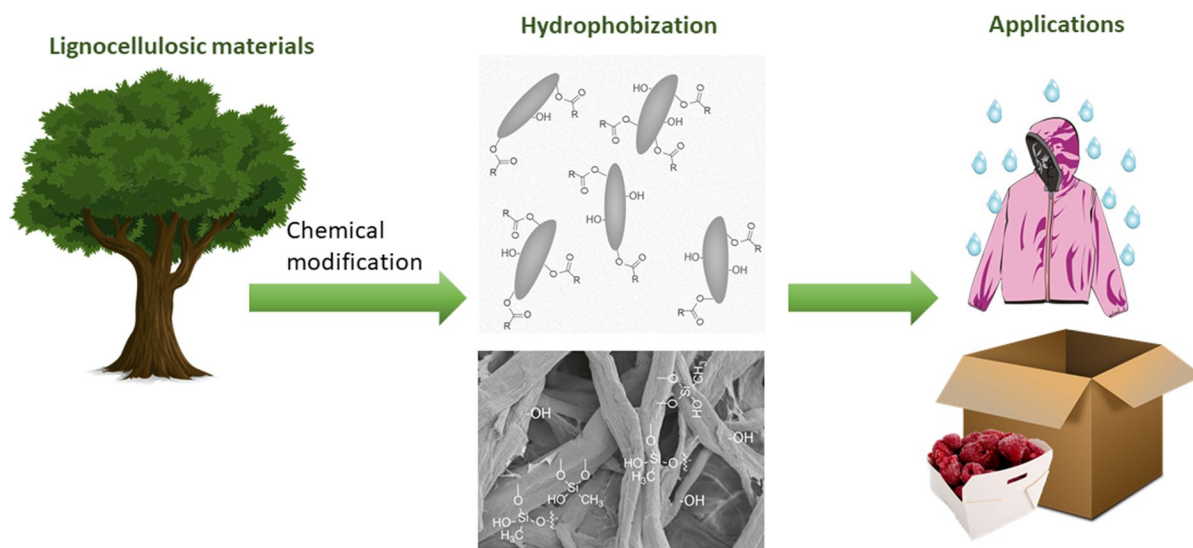
S. Rodríguez-Fabià (✉) · L. Johansson · K. Syverud
RISE PFI, Trondheim, Norway
e-mail: sandra.fabia@rise-pfi.no

J. Torstensen
Western Norway University of Applied Sciences, Bergen, Norway

K. Syverud
Department of Chemical Engineering, NTNU, Trondheim, Norway

Graphical abstract

Introduction

The packaging industry is the main plastic consumer, exceeding 140 million tons in 2017 (Ritchie and Rose 2018). Cellulose hydrophobization is regarded as one of the prerequisites for lignocellulosic materials to become plastic substituents, especially in packaging. Cellulosic materials are natively hydrophilic, but are still attractive and widely used for packaging applications. However, when used in the packaging of liquids, the cellulosic surface is coated with plastic (Schenker et al. 2021). This is not an optimal solution, especially for single-use containers, where the focus is on removing all plastic components. Therefore, it is paramount to develop hydrophobic cellulosic surfaces that are suitable for these applications. Cellulose is non-toxic, renewable, and biodegradable. In terms of chemical modification, cellulose molecules have many hydroxyl groups along the backbone that are potential sites for further chemical reactions. Grafting of both short molecules and polymers is possible, and the hydrophilic hydroxyl groups thus represent a great opportunity for hydrophobization (Dufresne 2013).

In the review *Hydrophobization of lignocellulosic materials part I: physical modification* (Rodríguez-Fabià et al. 2022a), physical hydrophobization methods were described. It was clear that both hydrophobicity and superhydrophobicity could be obtained, although the contact angles (CAs) were measured over a short period of time. The purpose of this review is to further discuss various molecular modifications that yield hydrophobic cellulose derivatives. As these methods all represent covalent modifications, they are evaluated as being more physically stable compared to adsorption and plasma methods discussed in the previous review (Rodríguez-Fabià et al. 2022a).

Characterization of substituted materials

The most common way to characterize the extent of the modification of lignocellulosic materials is the degree of substitution (DS). The DS represents the number of reacted hydroxyl groups per glucose residue and has a maximum value of 3.

Modification at the surface or in bulk?

In this set of reviews, we tried to classify the cited articles according to the loci of modification: either at the surface or in bulk. One should differentiate

between techniques that provide the surface DS and techniques that provide the bulk DS. Often in the literature this differentiation is not made, and therefore it is the reader's job to be aware of it.

This exercise has raised many questions from our side. In some cases, the authors clearly state whether the modification occurs at the surface or in bulk. In other cases, the DS is only measured at the surface (by XPS) or in bulk (by NMR). It is in these situations that questions arise. Could there also be bulk modification when the surface DS is high? Does a low bulk DS mean that the modification only occurs at the surface? In some examples, the change in crystallinity of the samples indicates where the modification takes place. In other examples, the variation in crystallinity might not be significant enough to provide an answer. Another question that comes to mind is which DS is the threshold between what we call surface and bulk modification. Clearly, a DS of 3 determined by NMR indicates full bulk modification, but what does a DS of 1.5 mean? So far, we have not been able to answer this question, although we imagine that there is a transition between what we consider a modification solely at the surface and a modification in bulk, and therefore there might be many stages that cannot be described either as purely surface or bulk modifications. However, in some cases, the crystallinity index can provide a good indication of where this modification occurs.

Crystallinity index

The crystallinity of lignocellulosic materials is a constantly debated subject. In brief, the crystallite type, size and relative presence are highly dependent on the natural source of the material (i. e. producing species) and the measurement principle/technique. Several methods exist for determining lignocellulosic crystallinity (Park et al. 2010).

Regardless of how to measure and define crystallinity, it is agreed that water cannot penetrate crystallites. Moreover, the loss of crystallinity is used as a sign that the hydrophobization is not only located on the surface but also in the bulk. However, as of yet, there is no clear connection between crystallinity reduction and the degree of bulk substitution. For example, Missoum et al. (2012) showed that fatty acid grafting on a nanocellulose surface and bulk may reduce crystallinity. Similarly, a reduction in crystallinity may also be seen with surface grafting of amorphous polymers (de Menezes et al. 2009), even though the change in crystallinity is due to the grafted polymer, not a change in the crystallinity of the substrate. This is summarized in Table 1.

Chemical hydrophobization techniques by molecule substitution

This review provides an overview of various modification techniques that are used for the hydrophobization of lignocellulosic materials. This review only includes chemical modification methods where "short" molecules are grafted. Modification by polymer grafting is described in the third part of this series of reviews (*Hydrophobization of lignocellulosic materials part III: modification with polymers* (Rodríguez-Fabià et al. 2022b)). An overview of the methods described in this review is given in

Table 1 Examples of crystallinity indexes calculated by X-ray spectroscopy and NMR before and after chemical modification. Wide-angle X-ray scattering (WAXS), X-ray diffraction (XRD)

Crystallinity before (%)	Crystallinity after (%)	Measurement technique	Substitution Method	Substitution type claimed by authors	Ref
81.4	80.9–72.4	WAXS	Esterification	Bulk and surface	Missoum et al. (2012)
54	46 and 57	XRD	Esterification	Surface	Sehaqui et al. (2017)
Ca. 80–90	Ca. 30–60	XRD	Polymer grafting The decrease in crystallinity is attributed to the amorphous grafted polymer	Surface	de Menezes et al. (2009)
90	89–83	XRD	Esterification	Surface	Lee et al. (2011)
35	Insignificant changes	XRD	Esterification	Surface	David et al. (2019)
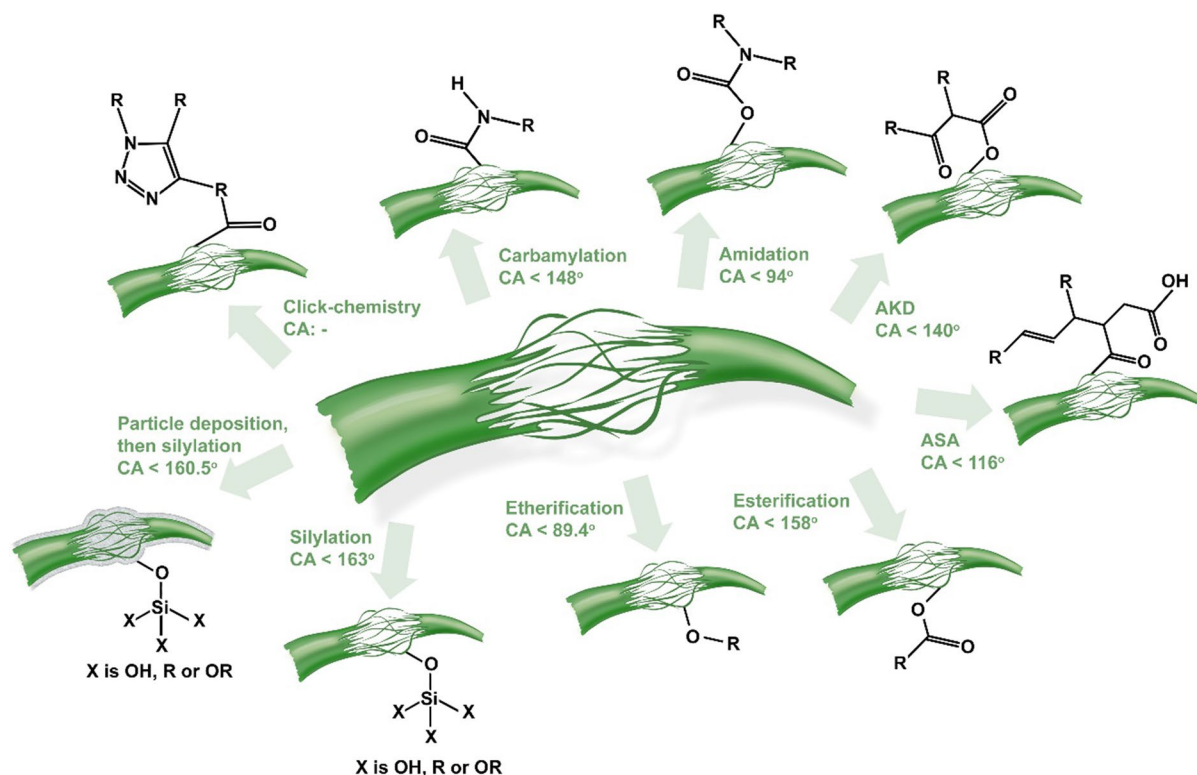
Fig. 1 The different hydrophobization methods discussed in this paper. The contact angles are the maximum angles found in our literature review. Amidation < 94° (Bendahou et al. 2015), alkyl ketene dimers (AKD) < 140° (Adenekan and Hutton-Prager 2019), alkenyl succinic anhydride (ASA) < 116° (Arancibia et al. 2021), carbamylation < 148° (Tursi et al. 2018), esterification < 158° (Geissler et al. 2013), etherification < 89.4° (Lee et al. 2020), silylation < 163° (Orsolini et al. 2018), particle deposition, then silylation < 160.5° (Sujing et al. 2010)
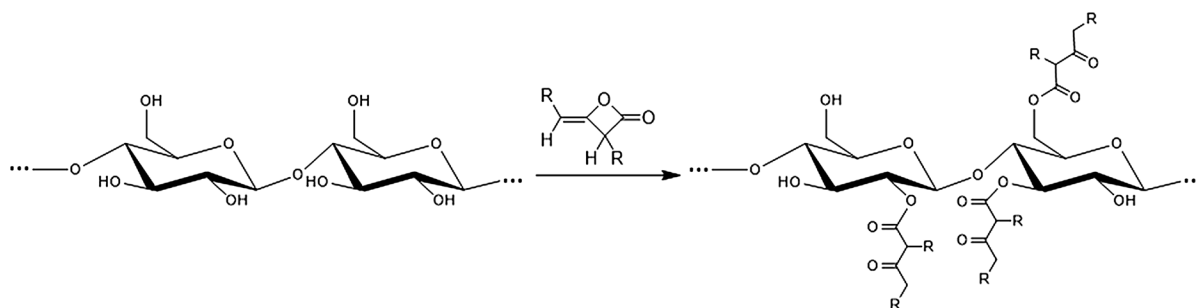
Fig. 2 Alkyl ketene dimers (AKDs) attach covalently to cellulose hydroxyl groups

Fig. 1, where the maximum contact angles reported here are also given. As mentioned in the introduction we tried to differentiate between bilk and surface modifications. Unless indicated otherwise in the text, the reader should consider that the modifications occur at the surface of the substrates.

The alkyl ketene dimer (AKD) and alkenyl succinic anhydride (ASA) method

Alkyl ketene dimers (AKDs) are oxetan-2-one derivatives, typically made by combining fatty acid and fatty acid chlorine derivatives (Fig. 2). These molecules

have been industrially applied to hydrophobize (or size) paper and cardboard since the 1950s (Downey 1953). AKD reacts with (hemi)cellulose, attaching a hydrophobic ester to the hydroxyl sites. AKD is typically prepared as an emulsion and subsequently added to the sheet-forming pulp before sheet formation. The AKD method has been reviewed by Lindström and Larsson (2008), highlighting the high number of variables and complexities that determine if AKD sizing is successful or not. Important factors that influence the success of AKD hydrophobization are listed below:

- Chemical structure of the AKD
- AKD distribution in the material
- Retention of AKD in the material
- The esterification reaction between AKD and (hemi)cellulose
- Hydrolysis of AKD during sizing

The five given factors are codependent. Typically, good retention is achieved by preparing a cationic AKD emulsion, which spreads and distributes well on the anionic cellulose surface. Shorter R-chains (R in Fig. 1) typically improve retention and distribution of AKD, due to their smaller size and less hydrophobic character. On the other hand, long fatty acid chains tend to increase the contact angle of the hydrophobized material. However, increased R length makes the AKD more viscous and hinders its diffusion within the cellulosic material.

Innovation in AKD sizing is a continuous process (Cunha and Gandini 2010). Recently, novel methods of impregnating materials with AKD using supercritical CO_2 have been used (Adenekan and Hutton-Prager 2019). The CO_2 pressure was found to be important at the beginning of impregnation. After 40 days, all contact angle values stabilized at 130°–140° compared to ~40° for the untreated sample. Russler et al. (2012) showed it was possible to achieve high AKD loading (>100%). Interestingly, these films displayed enhanced moisture sorption, indicating that AKD agglomeration and its interaction with cellulose may induce morphological changes facilitating water sorption.

Even though a lot is known about this technique, it seems that the obtained contact angles are highly variable, from about 100° (Li and Neivandt 2019) to 140° (Adenekan and Hutton-Prager 2019). Moreover, it seems to be unclear whether AKD binds cellulose by hydrogen bonding or covalently (Lindström and Larsson 2008; Adenekan and Hutton-Prager 2019; Li and Neivandt 2019). The importance of the type of binding is difficult to discern, as materials where the binding is believed to be electrostatic seemingly have a long lifetime and high contact angle (e. g. as in Adenekan and Hutton-Prager (2019)). The migration of AKD within the material over time indicates that the formation of covalent cellulose-AKD bonds is a slow process (Adenekan and Hutton-Prager 2019). Possibly, this varies depending on the impregnation method. For example, Li and Neivandt (2019) also observed a time-dependent increase in the contact angle. This evolution was temperature-dependent and was accelerated by higher temperature curing. They

Table 2 Overview of modifications of cellulosic materials by alkyl ketene dimers (AKDs) and alkenyl succinic anhydride (ASA)

Cellulose source	Type of cellulose	Hydrophobing agent	Contact angle (°)	Ref
Whatman filter paper no. 1	Fibers	AKD, Aquapel	<140	Adenekan and Hutton-Prager (2019)
Bacterial nanocellulose (BNC)	BNC	AKD, technical grade, Herkules	–	Russler et al. (2012)
Dissolving pulp	Fibers	AKD, technical grade, Herkules, 45% C16, 55% C18	<100	Li and Neivandt (2019)
Bleached kraft pulp hand-sheets	Fibers	ASA, Kemira	–	Lackinger et al. (2016)
Bleached kraft pulp (hard-wood) hand-sheets	Fibers	ASA	<110	Ashish et al. (2019)
Bleached pulp (enzymatically pretreated) hand-sheets	Fibers	ASA, BASF Basoplast 689	<116	Arancibia et al. (2021)
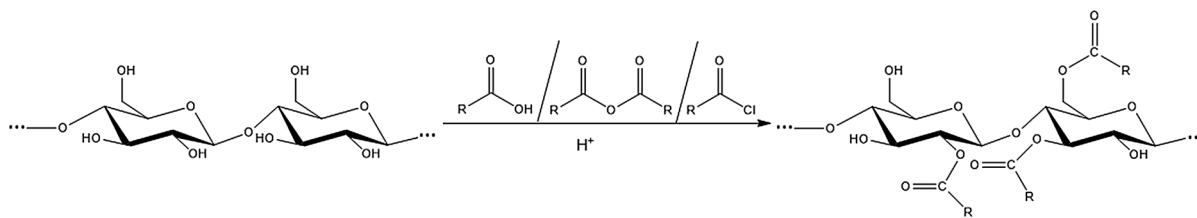
Fig. 3 Schematic representation of an esterification reaction

observed AKD agglomerates and hypothesized that at temperatures slightly above 50 °C (AKD melting temperature), AKD molecules are free to move, and distributed evenly across the cellulose surface. They found that heating below this temperature-induced the slowest evolution of the contact angle, reaching its maximum after 600 min. For curing temperatures above 50 °C, this time was shorter than 60 min. Comparing this with Adenekan and Hutton-Prager (2019), where samples were impregnated and then stored at ambient conditions, it is reasonable that the contact angle would settle after 140 days.

An alternative to AKD is alkenyl succinic anhydride (ASA), which may also be used as a paper sizing agent (Lackinger et al. 2016). Sizing by ASA is considered superior to AKD by some, as the kinetics are faster (Lackinger et al. 2016). Though faster, ASA is seemingly a somewhat poorer hydrophobing agent (CAs < 90°) compared to AKD (CAs < 100°) when compared experimentally on silica surfaces (Lindfors et al. 2007). The reason may be that ASA is easily hydrolyzed by water compared to AKD (Lindfors

et al. 2007; Ashish et al. 2019; Arancibia et al. 2021). The water stability of ASA has recently been investigated by Arancibia et al. (2021), improving it by adding CNF to the ASA suspension. Another possibility is preparing ASA and polyacrylamide emulsions, yielding contact angles above 100° for about 200 min in hand sheets prepared from cellulosic pulp (Ashish et al. 2019). An overview of the modifications by AKD and ASA is shown in Table 2.

Esterification

Esterification is one of the most used methods for cellulose hydrophobization via chemical modification. Esterification reactions occur between the hydroxyl groups of the cellulosic materials and either a carboxylic acid, an acid anhydride or an acyl chloride, introducing an ester group to the cellulose molecule (Fig. 3) (Missoum et al. 2013; Wang et al. 2018).

An important subgroup in the esterification reactions is acetylation reactions, which are used to introduce acetyl functional groups. The acetylation of
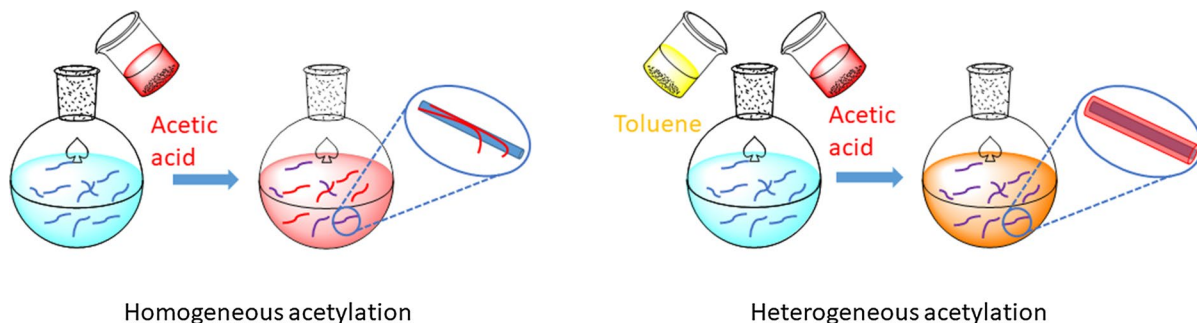
Fig. 4 Illustration of the homogeneous acetylation process (left) and heterogeneous acetylation process (right). In the homogeneous process, cellulose (blue) is dispersed the acetylation medium (here acetic acid). The acetylated molecules (red) become soluble in the acetylation medium and desorb from the substrate. The purple molecules represent chains that are par-

tially acetylated but are not soluble in the acetylation medium yet. In the heterogeneous process, a non-swelling diluent (toluene) is added to the acetylation medium (acetic acid), which ensures that the acetylated molecules (purple) are insoluble in the reaction medium, limiting the modification to the surface of the substrate

cellulosic materials (fibers, nanocelluloses) is typically performed by the reaction between the material and a dry mixture of acetic acid and acetic anhydride in presence of an acid catalyst (Habibi 2014). The substrates are either dry cellulosic materials or solvent-exchanged cellulose suspensions. Acetylation reactions can occur in homogeneous and heterogeneous media, as illustrated in Fig. 4. Homogeneous acetylation is performed in the acetylation medium, namely acetic acid or an acetic anhydride/acetic acid mixture, without the need of adding a diluent. As the reaction progresses, the surface cellulose molecules become soluble in the reaction medium as soon as they are sufficiently acetylated. This peeling-off effect leads to changes in the morphology of the (nano)fibers and allows the reaction to progress towards the core of the substrate until the (nano)fibers are completely acetylated and this results in a full dissolution of the substrate. On the other hand, reactions occurring in heterogeneous media, in the so-called "fibrous process", require the addition of a non-swelling diluent such as toluene, benzene or amyl acetate to the acetylation medium. In this case, the presence of the non-swelling agent allows the modified molecules to remain insoluble in the reaction medium and only the surface of the substrate is modified without affecting its morphology. Acetylation weakens the interchain hydrogen bonds, facilitating the desorption of the modified molecules (Tripathi et al. 2018). The resulting cellulose acetates are recovered by precipitation, usually in water or in aqueous acetic acid followed by washing with water (Sassi and Chanzy 1995; Habibi 2014; Wang et al. 2018). The DS of cellulose acetates has a strong impact on the physical properties of the polymer. Cellulose monoacetates are soluble in water, while diacetates are soluble in acetone and triacetates are insoluble in both acetone and water, but soluble in dichloromethane (Edgar 2004).

Surface modification

Some examples of acetylation reactions are listed here. For example, acetylation may be done directly on sheets formed by different pulps such as bleached and unbleached thermomechanical pulp (TMP) and chemi-thermomechanical pulp (CTMP) (Paulsson et al. 1994). This yielded two positive results. First and foremost, hydrophobization was achieved, although in this article the contact angles of the formed paper sheets were not measured; and secondly, the wet strength of the papers increased while the dry strength properties remained unchanged. This improvement in wet strength is most likely caused by a reduction in water sorption compared to unmodified sheets.

Sassi and Chanzy (1995) investigated heterogeneous and homogeneous acetylation of microcrystalline cellulose (MCC). They observed that with both acetylation processes the cellulose crystals are only modified at the surface, although a higher DS was achieved by homogeneous modification (DS = 2.81) than by heterogeneous modification (DS = 2.3). During homogeneous acetylation, the acetylated cellulose chains from the surface become soluble in the reaction media once they are sufficiently acetylated, leading to a decrease in the crystal thickness. In the fibrous process, only the surface chains were substituted, coating the unreacted core of the crystals. The diffraction patterns of the crystals showed that acetylation is an autoaccelerated process, meaning that chains that have started to react are more prone to reach a high DS.

Traditionally, acetylation of CNCs first involves the production of CNCs by hydrolysis of a cellulosic material with a strong acid, and then the acetylation reaction. This type of treatment leads to a decrease in crystallinity of the CNCs, although it improves their thermal properties (Abraham et al. 2016; Wu et al. 2018; Barbosa et al. 2019). This procedure has been widely used for the acetylation of cellulose and cellulose nanostructures (Sassi and Chanzy 1995). As an example, Barbosa et al. (2019) acetylated cellulose nanostructures obtained from hydrolysis of microcrystalline cellulose with sulfuric acid, and from hydrolysis with hydrochloric acid. Samples produced from sulfuric acid hydrolysis reached DS between 1.5 and 2.1 after acetylation with acetic acid/acetic anhydride, whereas samples from hydrochloric acid reached DS of 1.4–1.8. The variation in DS between both sets of samples was attributed to the different acidity of sulfuric and hydrochloric acids. After acetylation, the particle sizes of both sets of samples were more homogeneous and the acetylated nanostructures presented improved thermal properties. Xu et al. (2020) proposed a method to prepare acetylated CNCs from cellulose in one step. Microcrystalline cellulose was dispersed in acetic acid and reacted with acetic anhydride in presence of a catalytic

amount of sulfuric acid. As a result, a suspension of rod-like acetylated CNCs and acetylated cellulose was obtained. The two products were isolated by centrifugation, where the CNCs were the main product in the liquid phase, whereas acetylated cellulose formed a precipitate. The obtained CNCs had a crystallinity of ca. 70% and the highest DS that could be obtained was 0.42. Ávila Ramírez et al. (2017) conducted the acetylation of CNCs using acetic anhydride as both reagent and solvent medium and citric acid as catalyst. Two experiments were performed with different catalyst concentrations, which yielded DS of 0.18 and 0.34. The degree of crystallinity of the CNCs suggests that the nanocrystals were only modified at the surface. The modified CNCs were easily dispersed in chloroform, showing that after modification they had become more hydrophobic.

Recently, Beaumont et al. (2020) developed a novel acetylation approach for never-dried cellulose fibers using N-acetylimidazole. The reaction is not a typical esterification, but an acetyl transfer reaction. The reaction was performed on both bleached pulp (Cell) and an unbleached pulp (L-Cell). The reactivity of both samples was similar, although in the case of L-Cell there was a strong indication that mainly lignin and hemicellulose are modified. This method does not affect the crystallinity of the cellulose fibers and facilitates the fibrillation process, yielding acetylated CNF with a higher aspect ratio than non-modified CNFs. Films of acetylated cellulose CNFs presented contact angles of 50° compared to 39° for the unmodified films, while films of L-Cell presented increased contact angles from 58° to 73° after acetylation.

Other types of esterification reactions are also common. For example, cellulose fibers from various sugar cane bagasse pulping processes (Kraft pulping, organosolv ethanol/water and organosolv/supercritical carbon dioxide) and microcrystalline cellulose were modified with octadecanoyl chloride and dodecanoyl chloride (Pasquini et al. 2006). The contact angles of water, formamide, ethylene glycol and diiodomethane were measured and, in all cases, they increased after modification. In general, the substrates modified with octadecanoyl chloride displayed slightly higher contact angles than the corresponding samples modified with dodecanoyl chloride. An esterification reaction was also used to produce antibacterial cotton fabric via a two-step modification (Jantas and Górna 2006). First, the fabric was esterified

with chloroacetyl chloride, attaining a contact angle of 110°, and then the product was reacted with the potassium salt of 1-naphtylacetic acid. The final product had a contact angle of 122°.

In another work, Beaumont et al. (2021b,c) developed a C6-OH regioselective route for esterification of never-dried pulp. The reactions were performed in a water/acetone mixture in mild conditions using N-acylimidazoles that are generated in situ as hydrophobing agents. The modification was limited to the surface of the fibers and does not affect the physicochemical properties of cellulose fibers. CNFs were prepared from acetylated (C6AA), isobutyrylated (C6BA) and succinylated (C6SA) fibers. Films of C6AA and C6BA were prepared and showed an increase in contact angle (C6AA-CNF: 52°, C6BA-CNF: 61°) compared with unmodified CNFs (26°). Although the modified substrates were not hydrophobic, this synthetic route presents many advantages, particularly from the environmental point of view. The acetylation and isobutyrylation reactions can be performed with 50 wt% cellulose fibers, and they can be performed in mild conditions since it does not require water removal, solvent exchange or heating. In the case of succinylated fibers, the introduction of a C6-carboxylate group yields similar properties and degree of substitution as TEMPO modification, while still preserving the morphology of the fibers. Additionally, this modification also facilitates fibrillation of the sample, and the esterification reaction can be reversed by hydrolysis, yielding pristine cellulose with restored properties.

Heterogeneous surface esterification of bacterial nanocellulose (BNC) from Nata-de-coco was performed with several organic acids (acetic, hexanoic and dodecanoic acid) (Lee et al. 2011). The advancing and receding contact angles showed that with increasing chain length of the acid, the hydrophobicity of the surface increases and the DS decreases. The advancing contact angles of acetic, hexanoic and dodecanoic acid-modified substrates were 75°, 92° and 133°. The crystallinity of BNC remained approximately the same after modification, while the thermal stability decreased with increasing chain length of the grafted acid. BNC was modified by Ávila Ramírez et al. (2016) using acetic anhydride and citric acid as catalyst. Varying the reaction time, catalyst concentration and temperature yielded DS from 0.20 up to 0.73. At this DS range, the modification is only limited to the

surface. The water contact angles of BNC films with DS = 0, DS = 0.25 and DS 0.63 were 68°, 81° and 88°, respectively, showing an increase in hydrophobicity with increasing degree of substitution.

Esterification reactions have also been performed in ionic liquids. Bacterial and vegetable cellulose (VC) fibers were modified with a series of anhydrides of varying chain length, namely acetic, butyric and hexanoic anhydrides, as well as ASA and hexanoyl chloride (Tomé et al. 2011). The reactions were performed in tetradecyltrihexylphosphonium bis(trifluoromethylsulfonyl)imide [TDTHP][NTf$_2$]. The DS obtained for both types of cellulose ranged between 0.02 and 0.24. The fiber structure remained unchanged after esterification (verified by scanning electron microscope), meaning that the modification only occurred at the surface of the fibers. The samples modified with hexanoic anhydride and hexanoyl chloride displayed contact angles above 100° for both types of celluloses.

Müller et al. (2010) investigated the effect of three different esterification reactions on the swelling and conductivity of partially oxidized cellulose thin films. Methylation yielded the lowest conversion of COOH groups because it selectively reacted with C6-COOH, resulting in a small decrease in conductivity and swelling. Both thermally activated esterification and carbodiimide activated esterification provided higher conversion than methylation, where carbodiimide activation almost reached full conversion. These two reaction methods formed covalent ester cross-links that resulted in a reduction of the swelling of the films. The authors concluded that the change in the physical properties of the films after drying (hornification), was not caused by the packing of the cellulose chains, but by the esterification reaction.

So far in this review, only esterification reactions performed in liquid medium have been reported. Gas-phase esterification is an interesting technique because it does not involve the extensive use of solvents and facilitates the rinsing of the samples. Modification of cellulosic materials performed in liquid media has the disadvantage that neither the modifying agent nor the modified fibers are soluble in water,
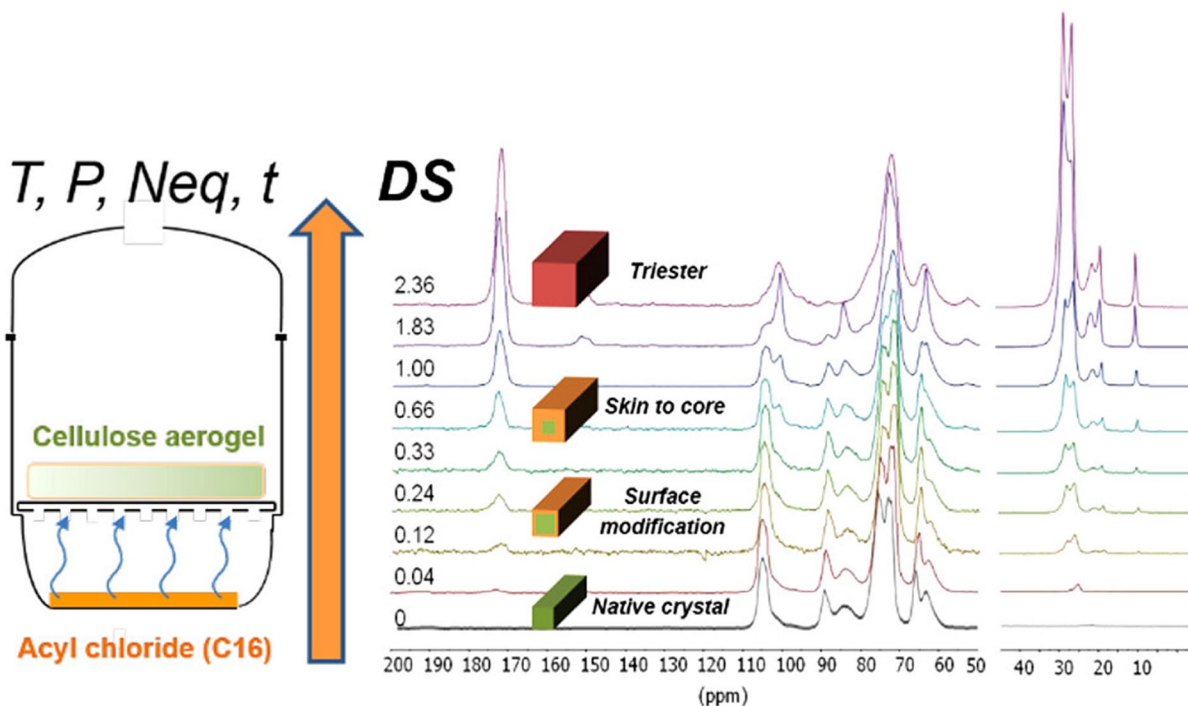
Fig. 5 Schematic representation of the propagation of the acylation reaction with increasing degree of substitution. Image reproduced from Fumagalli et al. (2013a). The ^{13}C NMR spectra show the evolution of the ester linkage carbonyl signal (172 ppm) and the aliphatic carbons from the fatty tail of the reagent (40–10 ppm). The crystal figures show how the esterification occurs first at the surface hydroxyls of cellulose and then propagates to the crystalline core

while cellulose fibers often contain large amounts of water. Therefore, it is necessary to add an apolar solvent to perform these reactions. Gas-phase reactions avoid the solubility problems between the various components in the reaction, resulting in a simpler process that requires fewer chemicals. Gas-phase esterification was performed on filter paper and tunicate by Yuan et al. (2005). Filter paper was treated with acetic acid (AcOH)/ trifluoroacetic anhydride (TFAA) and acetic anhydride (Ac$_2$O)/TFAA. Contact angles above 90° were obtained. The samples were kept at 50% relative humidity for 3 months and they maintained the hydrophobic properties. Ac$_2$O/TFAA treated samples immersed in water for 3 min lost their hydrophobic properties, while the AcOH/TFAA treated samples remained the same. For Ac$_2$O/TFAA, no DS could be detected. Tunicate samples presented higher DS than filter paper due to the larger surface area of the fibers. Microfibrillated cellulose (MFC) films were also modified with mixtures of trifluoroacetic anhydride with either acetic anhydride or acetic acid (Rodionova et al. 2013). The water contact angle of the esterified MFC films increased, reaching the highest value (96.9°) when a 1:1 Ac$_2$O/TFAA mixture was used at 30 °C. The effect of different purification methods was also investigated, showing that washing the films with diethyl ether led to an increase in the hydrophobicity of most of the samples.

Palmitoyl chloride was successfully grafted onto micrometre-size cellulose particles by gas-phase esterification. The DS increased with increasing reaction time and temperature (David et al. 2019). The modification did not significantly affect the crystallinity of the particles; however, it made them more hydrophobic. Water contact angles increased from 44° to 98°–109° after esterification. The contact angles of other apolar liquids were also measured and showed that the particles had become slightly lipophobic. The surface of MFC and cellulose nanocrystal aerogels was also modified with palmitoyl chloride using gas-phase esterification (Fumagalli et al. 2013a, b). The authors obtained aerogels with several DS by varying the experimental conditions (reagent quantity, temperature, pressure and reaction time). In the case of MFC aerogels, the DS ranged from 0.04 to 2.36, while for CNC-aerogels, the DS ranged from 0.07 to 2.50 (Fig. 5). At lower DS the aerogels are only modified at the surface, but the esterification progresses from the surface towards the core as

the DS increases, until the microfibrils/nanocrystals are fully substituted and are converted into cellulose tripalmitate. At low DS the surface consists of cellulose tripalmitate even though the crystalline core is preserved. The comparison of the efficiency of gas esterification of CNC-aerogels with esterification in liquid medium of a CNC suspension showed that both methods allowed the tunability of the DS to the same extent and affected the morphology of the CNCs in the same manner (Fumagalli et al. 2013b).

Further work was performed to compare the gas-phase esterification of MFC aerogels using palmitoyl chloride, decanoyl chloride, and the two bifunctional compounds sebacoyl chloride and (2-dodecen-1-yl) succinic anhydride (Fumagalli et al. 2015). Decanoyl chloride displayed similar behaviour to palmitoyl chloride, both reaching a DS around 1 and the esterification of MFC occurred from the surface to the core. A much lower DS (around 0.14) was achieved with the two bifunctional compounds and the modification was limited to the surface of the microfibrils. Transesterification reactions were used to modify CNCs with vinyl acetate (Çetin et al. 2009), and with canola oil fatty acid methyl esters (Wei et al. 2017). Vinyl acetate modified samples which had reacted for over 2 h formed stable suspensions in tetrahydrofuran (THF), indicating that the hydrophobicity of the samples had increased. CNCs modified with canola oil displayed improved thermal stability compared to the unmodified ones with an increase in the temperature of maximum decomposition rate of 28 °C. The water contact angle of the CNCs increased from 23° to 68° after surface modification.

Ball milling has also been used as a method for the esterification of cellulosic materials. Huang et al. (2012) esterified cellulose powder with hexanoyl chloride in N, N-dimethylformamide (DMF). The process resulted in a suspension of cellulose nanofibers esterified at the surface. The authors confirmed that simultaneous milling and addition of hexanoyl chloride resulted in the highest weight gain of the samples (35%), while preserving the crystallinity of the samples, compared with ball milling in dry conditions, which yields amorphous cellulose. Rao et al. (2015) conducted the esterification of cellulose powder in a ball mill together with pentafluorobenzoyl chloride and pyridine. The modifications were performed in either toluene or DMF. Complete esterification of the surface of nanofibers was obtained in

DMF, and the esterification contributed to the separation of nanofibers that were hydrogen-bonded. On the other hand, the sample treated in toluene consisted of dense flakes, which are tightly packed nanofibers. The combination of milling with esterification preserved the crystalline structure of the samples. The contact angles of cellulose modified in DMF and toluene were 102.7° and 133°, respectively. In a recent publication, Beaumont et al. (2021a) performed the esterification of cellulose in solid state by taking advantage of the surface-confined water present in cellulose fibers. The acetylation reaction was performed with *N*-acetylimidazole and catalyzed by imidazole. The presence of 7 wt% water in the fibers increased both the reaction rate and the efficiency. The acetylation process did not affect the fiber structure, and the water contact angle of the fibers increased from 12° to ~ 134°. Interestingly, increasing the water content to up to 30% had a detrimental effect on the reaction efficiency, but increased the selectivity for the modification of C6-OH.

Bulk modification

Acetylation reactions are also performed as bulk modifications. For example, Li et al. (2019) acetylated CNCs. The CNCs were dispersed in anhydrous pyridine, and then a mixture of acetic anhydride and anhydrous pyridine was added to the CNC suspension. The CNCs reached a DS of 2.16. The resulting acetylated nanocrystals lost the crystalline structure forming a network and were used in bionanocomposites with poly (3-hydroxybutyrate-co-3-hydroxyhexanoate) (PHBH). These composites presented improvements in the mechanical properties as well as water and oxygen barrier properties compared with unmodified CNC/PHBH composites.

Cellulose from viscose rayon, bleached sulphite pulp and cotton linter was acetylated in p-toluenesulfonyl chloride (Shimizu and Hayashi 1988). Rayon reached a DS of 3 after a few hours, whereas pulp and linter reached DS of 2.44 and 2.10 after 20 h. The difference in the DS between the three materials is probably caused by differences in the crystallinity and the degree of polymerization of the fibers. Mecerization of cotton linter and pulp before esterification resulted in an increase of the DS to almost 3. The same reaction system was used by Jandura et al. (2000), who esterified cellulose from highly purified bleached sulphite pulp with a series of long-chain organic acids, namely undecylenic acid, undecanoic acid, oleic acid, and stearic acid. They observed that the DS increased substantially when the reaction time was increased from 1 to 2 h. Overall, they obtained DS between 0.08 and 1.11.

Kenaf fibers were acetylated with acetic anhydride in pyridine, and after acetylation, the cellulose nanofibers (CNFs) were isolated by mechanical treatments (Jonoobi et al. 2010). After esterification, the crystallinity of both the fibers and nanofibers decreased slightly. The contact angles of acetylated fiber and nanofiber networks were 113° and 115°, respectively. Similarly, cellulose from wheat fibers was modified with succinic, maleic and phthalic anhydrides (Sehaqui et al. 2017). After esterification, the fibers were disintegrated in a microfluidizer resulting in CNFs. Succinic anhydride modified fibers (SCNFs) achieved a DS of 0.67. Maleic and
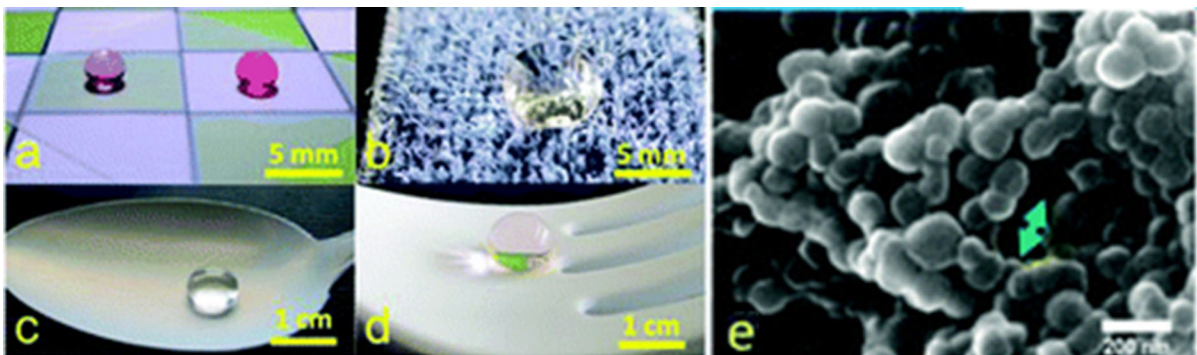
Fig. 6 Cellulose stearoyl ester (CSE) hydrophobic coating on **a** glass, **b** cloth, **c** metal and **d** plastic, **e** scanning electron microscope (SEM) image of a superhydrophobic CSE film. Image adapted from Geissler et al. (2013)

phthalic anhydride modified CNFs achieved a DS of 0.15 and 0.17, respectively. The thermal stability of the esterified fibers was lower than that of unmodified fibers, even though they presented better stability than TEMPO (2,2,6,6-tetramethylpiperidin-1-yl)oxyl) oxidized fibers.

Cellulose from Posidonia biomass was esterified with succinic, maleic and phthalic anhydrides using microwave power (Chadlia and Farouk 2011). The effects of the choice of catalyst and its concentration, power, anhydride concentration and reaction time on the DS were investigated. A wide range of DS was obtained up to 2.25. The presence of organic catalysts yielded products with the highest DS. These results were compared with the results obtained from conventional esterification reactions and showed that twice as high DS are obtained with microwave heating, in addition to much shorter reaction times (from hours to minutes).

Superhydrophobic cellulose stearoyl ester (CSE) films were prepared by Geissler et al. (2013) by esterification of MCC with stearoyl chloride (Fig. 6). CSE nano- and microparticles with a DS of 2.95 were obtained via nanoprecipitation of CSE. The contact angles of water and glycerol on CSE films were found to be 158°. In addition, rough microparticles were prepared by aggregation of nanostructures at the surface of the particles. Both the nanostructured and nano-/microstructured films displayed a high water repellency (~ 0.05 m s^{-1}), self-cleaning properties, and showed stability in air for more than 2 months, and in water above 96 h.

Microcrystalline cellulose was modified with vinyl laurate in 1-allyl-3-methylimidazolium chloride via transesterification (Wen et al. 2017). By varying the reaction conditions, the DS could be tuned, resulting in films with contact angles between 96.3° and 120.7°. The crystalline structure was lost upon esterification, but the thermal stability was improved.

Looking at the esterification techniques reported in this review, one can see a clear trend towards green chemistry. One of the first steps towards more environmentally friendly chemistry was the use of gas-phase reactions (Yuan et al. 2005; Fumagalli et al. 2013a), which avoids the need for solvent exchange, a process that requires excessive use of solvents. In the last couple of years, new esterification approaches have been reported, which can be performed in never-dried substrates under mild conditions (Beaumont et al. 2021a, b). This avoids both the drying and solvent exchange stages and can be realized by using confined surface water (Beaumont et al. 2021a). This is an important first step to implementing modification routes that not only limit the use of chemicals, but also reduce the energy requirements of the process. Additionally, recent publications also show a tendency towards limiting the modifications to the surface, thus preserving the physical properties of the substrates. For detailed information about the esterification of cellulose and nanocellulose, the reader is referred to the review by Wang et al. (2018). Table 1 in the supplementary information (SI-Table 1) provides a summary of all the modifications by esterification listed above.

Etherification

Etherification reactions create ether bonds at the hydroxyl groups of cellulosic materials and, when performed in heterogeneous conditions, require the activation of the hydroxyl groups with a base, which weakens the hydrogen bonds between the polymer chains and makes them more accessible when they are in suspension (Fig. 7). The etherifying agents are alkyl/silyl chlorides or bromides, oxiranes, or vinyl compounds (Heinze et al. 2018). Etherification reactions in general are not specific to a certain hydroxyl group (Habibi 2014; Kargarzadeh et al. 2018). Like esterification, etherification can be limited to the
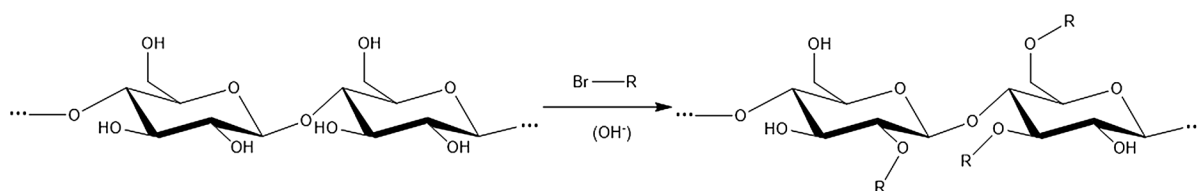
Fig. 7 Schematic representation of an etherification reaction with an alkyl bromide

Table 3 Overview of modifications of cellulosic materials by etherification. Microcrystalline cellulose (MCC), cellulose nanocrystal (CNC)

Cellulose source	Type of cellulose	Etherification agent	Degree of substitution	Contact angle (°)	Ref
Surface					
MCC	CNC	1-bromodecane	2.6	89.4	Lee et al. (2020)
		Ac$_2$O*	2.4	78.3	
Bulk					
	MCC	Benzyl chloride	0.29–0.54		Li et al. (2011)
	MCC	1-bromooctane		74.3	Bae and Kim (2015)
		1-bromodecane		84.9	

*Acetylation. Results reported for comparative reasons

surface. An advantage of etherification over esterification is that it is a more regioselective reaction for the substitution of C6 (Fox et al. 2011).

Surface modification

Modification of CNCs by etherification was compared with acetylation (Lee et al. 2020). Etherification was performed with 1-bromodecane and acetylation with acetic anhydride. The water contact angles of the acetyl-CNCs (resulting from the acetylation reaction) and alkyl-CNCs (resulting from the etherification reaction) were 78.3° and 89.4°. The thermal stability of CNC/PLA composites improved, particularly in the case of alkyl-CNCs. In addition, small concentrations of alkyl-CNCs improved the mechanical properties and gas barrier properties of the composites.

Bulk modification

Etherification of microcrystalline cellulose was performed with benzyl chloride (Li et al. 2011). Benzylcellulose with DS between 0.29 and 0.54 was obtained, and the DS increased with increasing temperature and benzyl chloride concentration. The increase in DS also favoured the solubility/dispersibility in organic solvents. The benzylation reaction resulted in the formation of amorphous cellulose particles and a decrease in thermal stability. Microcrystalline cellulose was modified with octyl and dodecyl alkyl chains to improve its compatibility with polymers such as poly(lactic acid) (PLA) (Bae and

Kim 2015). The water contact angle of octyl ether cellulose was 74.3° and the one of dodecyl ether cellulose was 84.9°. The hydrophobicity of the samples increased with the length of the alkyl chain. The thermal stability of the modified cellulose decreased with respect to the unmodified one. PLA composites were prepared with both cellulose ethers and they presented improved thermal properties because the crystallization temperature of the films decreased, and the crystalline regions have higher thermal stability than the amorphous regions. The tensile strength increased by 13.0% for octyl ester/PLA composites and 10.2% for dodecyl ester/PLA composites. Modifications by this method are shown in Table 3.

Silylation

Silylation is the reaction between nucleophilic groups such as alcohols, carboxylic acids and amines, with silyl groups (R$_3$Si-). Silylation is used to graft molecules to cellulose and its derivatives via covalent bonds (Missoum et al. 2013; Kargarzadeh et al. 2018). The reaction requires the presence of water and involves three steps: (1) hydrolysis of the silane molecules to the corresponding silanols (R$_3$Si-OH) in the presence of water, (2) adsorption of the silanols onto cellulose surfaces by hydrogen bonding, and (3) self-condensation of the silanols into a siloxane network and condensation of the siloxanes with cellulose by thermal treatment. The grafted silanes can form various structures, depending on the experimental conditions and the number of hydrolyzable substituents in the molecule. Common hydrolyzable groups in silane molecules are -Cl, -OR, -NMe$_2$ (Fadeev
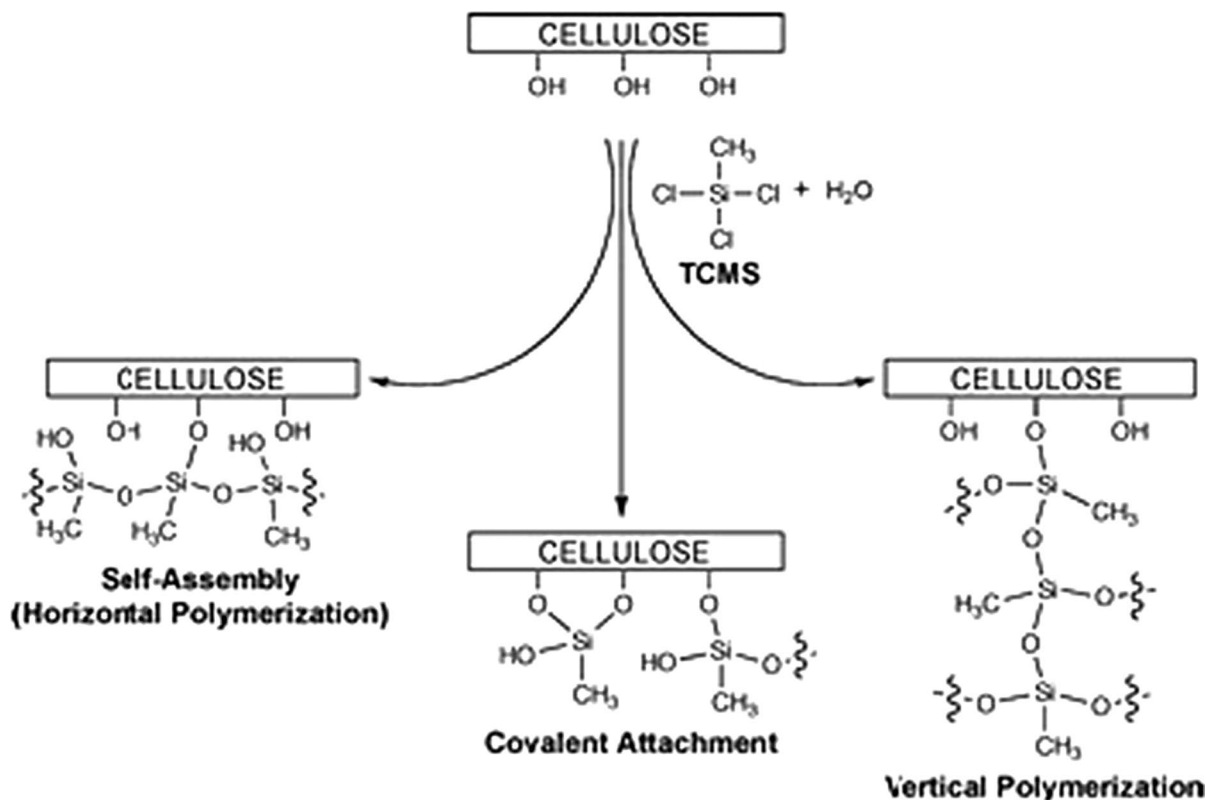
Fig. 8 Schematic representation of the potential constructs formed by grafting of trichloromethylsilane (TCMS). Image reproduced from Cunha and Gandini (2010)
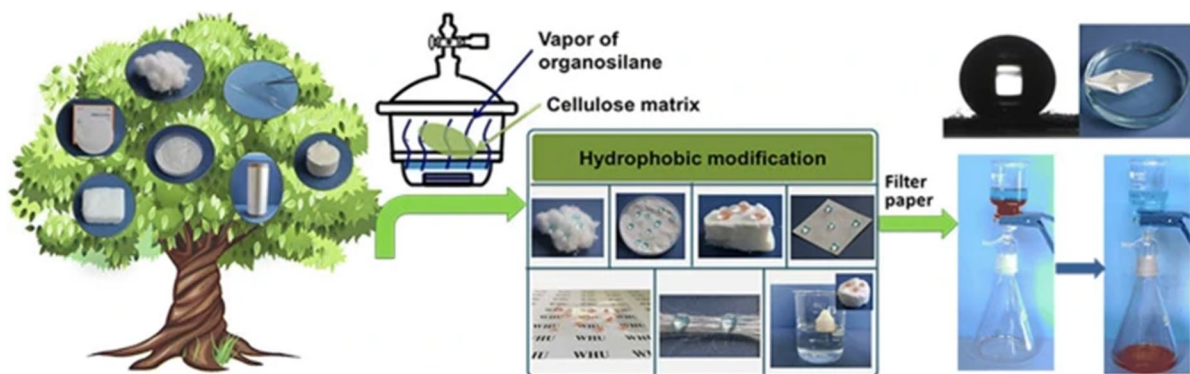
Fig. 9 Hydrophobization of various cellulosic materials by vapor deposition. Image obtained from Yu et al. (2019)

and McCarthy 2000; Andresen et al. 2007). Figure 8 shows three possible architectures of the grafted silanes, which can polymerize in the horizontal direction (self-assembly), covalently react with one or more hydroxyl groups (covalent attachment), or polymerize in the vertical direction (vertical polymerization) (Cunha and Gandini 2010). Monofunctional silanes (with only one hydrolyzable group) can only be grafted to the surface through covalent attachment, while difunctional silanes (two hydrolysable groups)

can be grafted by both covalent attachment and vertical polymerization. Lastly, trifunctional silanes (three hydrolyzable groups) can be grafted by the three modalities shown in Fig. 8. The polymerization of trifunctional silanes into 3-D siloxanes is the most common process when there is sufficient water in the system (Fadeev and McCarthy 2000).
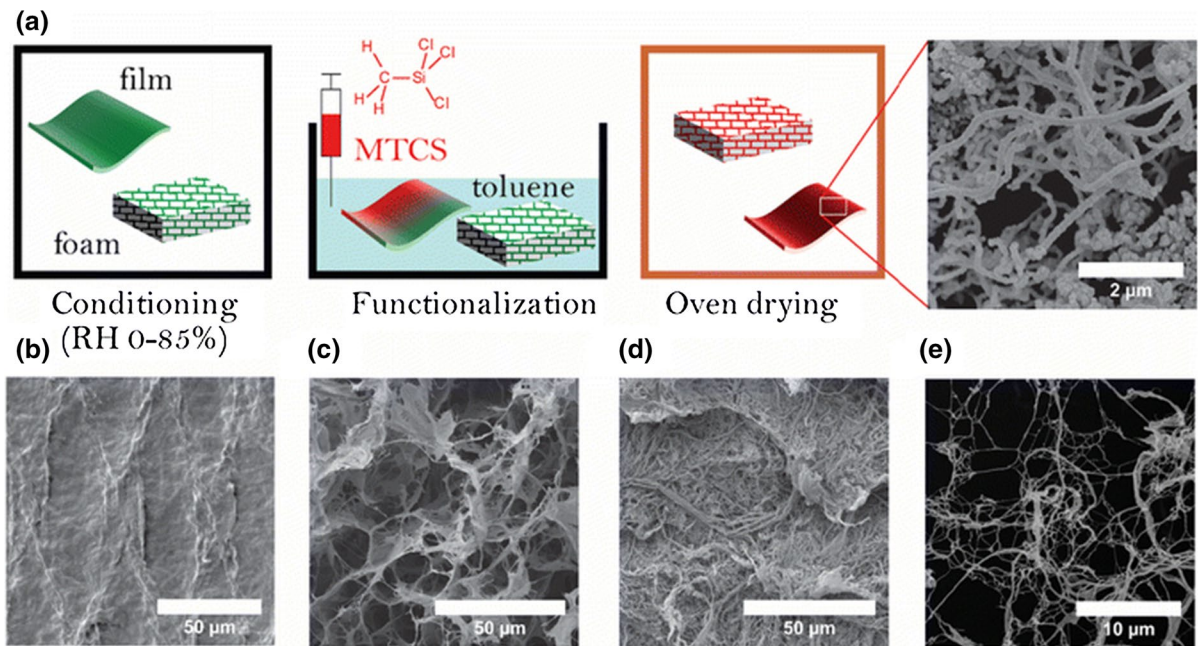
Surface modification

Gas-phase reactions are often used in modifications with silanes. A simple, solvent-free method was used to modify filter paper with trichloromethylsilane (TCMS) via a gas–solid phase reaction performed at ambient conditions (Cunha et al. 2010). The water contact angles of the successfully modified substrates were 125°, 134° and 136°. The water contact angles increased with increasing reaction time between the paper and TCMS. The contact angles of glycerol, diiodomethane and 1-bromonaphtalenate were also measured and showed that the modified papers were both hydrophobic and lipophobic. The biphobic properties of the modified papers are partly due to the increase in surface roughness by the formation of silica particles on top of the fibers.

A similar gas-phase modification approach was used by Yu et al. (2019) (Fig. 9). Filter paper, MCC, viscose rayon film, regenerated cellulose film, CNC aerogel and BNC were modified with a series of organosilanes, namely methyltrimethoxysilane (MTMS), hexamethyldisilazane (HMDS), *n*-dodecyltrimethoxysilane (*n*-DDTS), and perfluorooctyltriethoxysilane (PFTS). The contact angles varied depending on the substrate and the chosen organosilane. Filter paper, CNC aerogel, regenerated cellulose, and MCC achieved the highest contact angles when they reacted with PFTS, which were 146°, 136°, 120°, and 133°, respectively. The highest contact angle of viscose rayon was achieved when it reacted with HMDS and of BNC when it reacted with *n*-DDTS, and the values were 147° and 136°, respectively. The same method was applied for the dynamic modification of viscose rayon, yielding a water contact angle of 132°. Cotton fabric woven from this modified rayon maintained the hydrophobic properties of the viscose rayon. The water uptake of the PFTS-modified paper decreased to below 40%, and the modified paper was used for oil/water separation with an efficiency above 99%. Jarrah et al. (2018) used the same procedure to modify cotton

fibers with four different trichloroalkylsilanes (TCMS, dichlorodimethyl silane, butyltrichlorosilane (BTCS) and trichloro(3,3,3-trifluoropropyl)silane). The contact angles of the modified samples were 101°, 97°, 110°, and 59°, respectively. CH_3Si-modified samples were tested as adsorbents for hexadecane and crude oil. After the modification, the adsorption capacity of hexane increased from 2.7 to 12.7 g/g, and the one of crude oil from 6.8 to 15.4 g/g.

The surface of MFC films from bleached and unbleached pulp as well as carboxymethylated bleached and unbleached pulp was modified with HMDS via a gas-phase reaction (Chinga-Carrasco et al. 2012). The water contact angles of the unmodified films ranged between 38° and 74° and increased to 88°–101° after modification with HMDS. The results showed that bleached MFC films presented a larger increase in contact angle than unbleached films. In the cases where the coverage of the films with HMDS is sufficient, the roughness of the surfaces contributes to increasing the hydrophobicity. The hydrophobized films made of carboxymetylated cellulose presented oxygen permeabilities below 0.06 mL mm m^{-2} day^{-1} atm^{-1}, which are interesting for packaging applications. See Table 3 in the supplementary information for oxygen permeability values of cellulosic and plastic materials.

Although there are many examples of gas-phase modifications with silanes, it is still common to perform these reactions in liquid media. All the examples listed below are liquid-based reactions. Tang et al. (2016) coated paper samples with alkyltrichlorosilanes of different chain lengths: TCMS, BTCS, dodecyltrichlorosilane and octadecyltrichlorosilane. Water, ethylene glycol and diiodomethane contact angles were measured on the modified surfaces, which displayed hydrophobic as well as moderately lipophobic behavior. TCMS-modified substrates displayed the highest contact angles for all solvents. In the case of water, the contact angles ranged from approximately 120°–150°. The water contact angle of TCMS-grafted samples was higher than the one reported by Cunha et al. (2010) because in this case the paper was coated by immersion, leading to a higher density of nanostructures than vapor deposition. Ly et al. (2010) modified filter paper and commercial microcrystalline cellulose (Avicel) with two different agents: 3,3,3-trifluoropropyl trimethoxysilane (TFPS) and 1H,1H,2H,2H-perfluorooctyl

Fig. 10 a Schematic representation of the modification of cellulose nanofiber films and foams with trichloromethylsilane. Scanning electron microscope images of b a dense film, c a foam, d a porous film and e suspended nanocellulose. Image obtained from Orsolini et al. (2018)
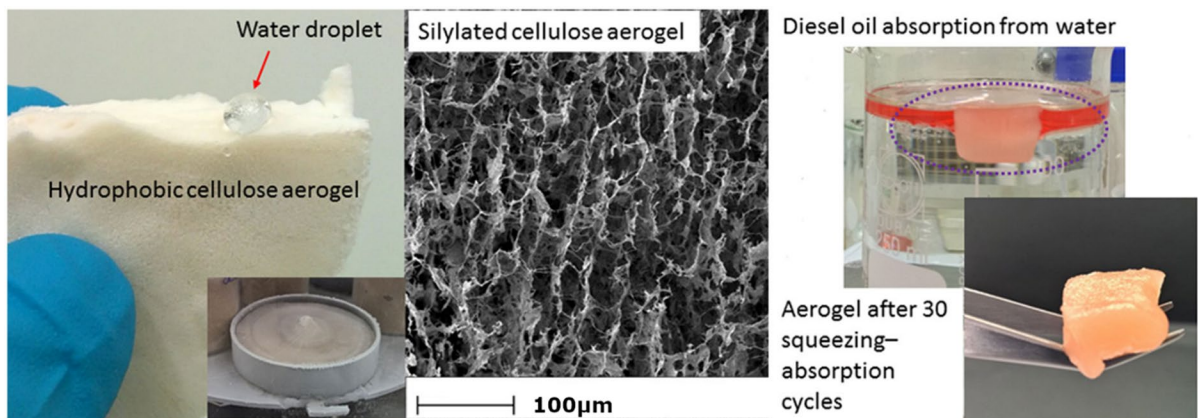
Fig. 11 Hydrophobic cellulose nanofiber aerogels for oil sorption applications. Image obtained from Laitinen et al. (2017)

trimethoxysilane (PFOTMS). The resulting contact angles were 116° and 129° for filter paper, and 115° and 125° for Avicel. In both cases, the highest contact angles were achieved with PFOTMS coatings.

MFC was modified with chlorodimethyl isopropylsilane (CDMIPS) (Goussé et al. 2004; Andresen et al. 2006). The contact angles of samples with varying DS increased from 28° for the unmodified sample to up to 146° for the modified ones. High contact angles were obtained even with low DS, indicating that the surface roughness played an important role in increasing the hydrophobicity of the sample. The modified cellulose was further used as an emulsion stabilizer for water-in-toluene emulsions (Andresen and Stenius 2007).

Both dense and porous CNF films and CNF aerogels were modified with TCMS as shown in Fig. 10

(Orsolini et al. 2018). The CNF substrates were pre-conditioned for 10 days and then dipped into a solution of TCMS in toluene. Polysiloxane filaments were formed at the surface of the films and within the macropores of the aerogels. Dense films presented superhydrophobic properties with advancing and receding contact angles between 150° and 160°. Similar values were obtained for porous films, where the advancing contact angles were between 157° and 163°, and the receding ones reached 150°. The aerogels were primarily modified at the surface, and they could retain dodecane. The dodecane retention ability of the aerogels as well as their mechanical properties

remained unchanged after 6 cycles. Suspended CNFs were also modified with TCMS. The dried modified CNFs resulted in a powder with high water repellency and the ability to retain dodecane.

Laitinen et al. (2017) prepared CNF aerogels from recycled box board, recycled milk container board, fluting board, and industrially bleached birch kraft pulp (Fig. 11). The nanofibers were mixed separately with methyltrimethoxysilane and hexa-decyltrimethoxysilane solutions before preparing the aerogels. The water contact angles of kraft pulp, fluting board, box board and milk container board aerogels were 142.9°, 159.0°, 107.2°, and 129.4°,
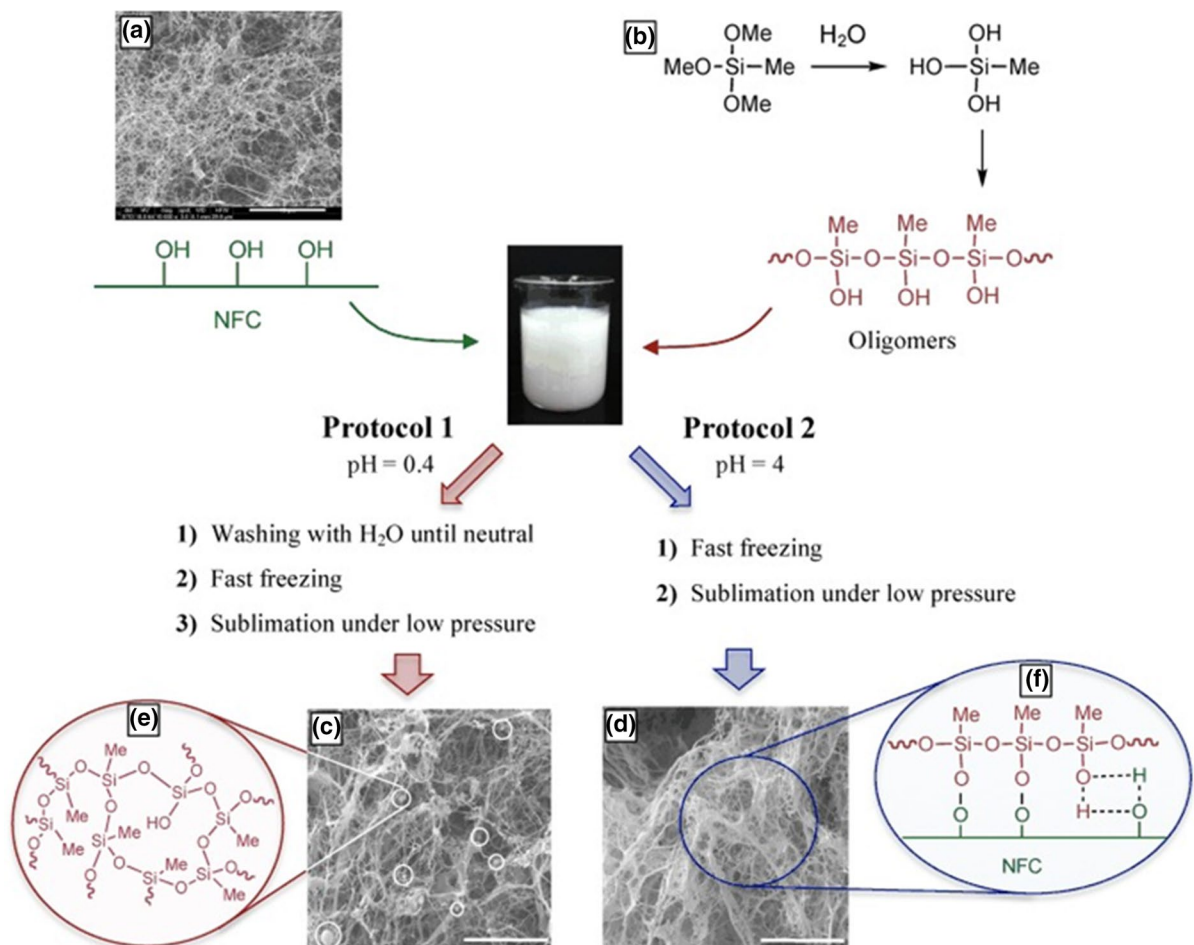
Fig. 12 Scheme of the two methods used for the silylation of nanofibrillated cellulose (NFC). **a** Scanning electron microscope (SEM) micrograph of NFC from oat straw pulp, **b** hydrolysis/condensation of methyltrimethoxysilane, **c** SEM micrograph of NFC silylated according to protocol 1, **d** SEM micrograph of NFC silylated according to protocol 2, **e** polysiloxane formed by condensation, **f** condensation and/or hydrogen bonding between the oligomers and the NFC surface. Image obtained from Zhang et al. (2015)

respectively. The diesel oil sorption of the aerogels increased with higher porosity and lower density of the aerogel. The absorption of various oils and organic solvents was also tested. The aerogels could be reused, retaining over 70% of their absorption capacity after 30 absorption/squeezing cycles. There are many reports of silane-modified nanocellulose aerogels with oil-absorbing properties. For instance, aerogels modified with hexadecyltrimethoxysilane (Rafieian et al. 2018), methyltrimethoxysilane (Zhang et al. 2014; Feng et al. 2015; Cheng et al. 2017; Lazzari et al. 2017), fluorinated silanes (Jin et al. 2011), and trimethylchlorosilane (Sai et al. 2015) have also been developed for this purpose.

In another study, CNF films were first activated by UV/O_3 cleaning and then modified by either HMDS or (3-aminopropyl)-trimethoxysilane (APTES) (Peresin et al. 2017). The DS was higher in the pre-treated films than in non-activated films used as reference. The contact angles of APTES and HMDS modified films were ca. 60° and 70°, respectively. The oxygen permeability of the films increased after modification with HMDS, while it decreased after modification with APTES. Zhang et al. (2015) modified CNFs with methyltrimethoxysilane following two different protocols: the first one formed polysiloxane particles

that were dispersed within the CNFs, and the second one formed a polysiloxane coating on top of the nanofibers (Fig. 12). CNFs modified with protocol 1 absorbed water, whereas CNFs modified with protocol 2 displayed contact angles between 110° and 147°. Fibers treated with protocol 2 displayed an improvement in their thermal stability, and when incorporated into a polydimethylsiloxane matrix, they also improved the mechanical properties of the composite.

The surface of bacterial nanocellulose was modified with methyltrimethoxysilane (MTMS) by Kono et al. (2020) using a reaction performed in water. By varying the amount of silane added to the reaction, the authors obtained degrees of molar substitution (MS) ranging between 0.41 and 5.90. The degree of molar substitution is defined as the number of MTMS molecules reacted per glucose residue, and in this case, it can result in values higher than 3 due to the polymerization of MTMS. The optimal degree of molar substitution was found to be 0.66 because at that MS the molecular mobility and hydrophobicity of the nanofibers are optimized. Above an MS of 0.66, the hydrophobicity of BNC increases at the expense of molecular mobility. The characterization approach reported in this work can be useful to provide an insight into how chemical modifications
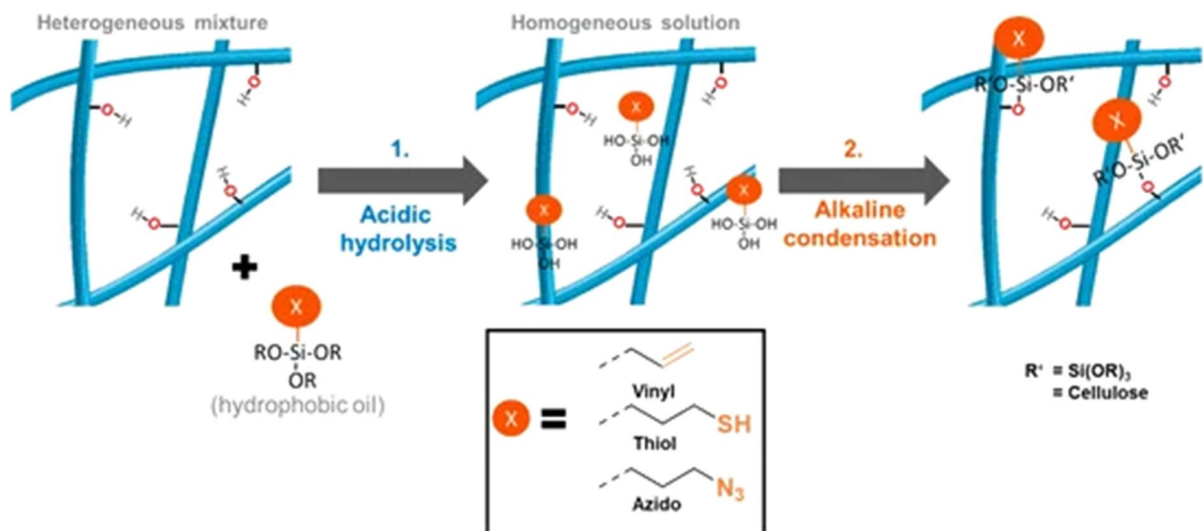
Fig. 13 Schematic representation of the silanization protocol. (1) The reaction mixture is acidified with HCl and the alkoxysilane is hydrolyzed. (2) Addition of NaOH leads to a condensation reaction between the substrate and the silanols. Following this procedure, azide, vinyl and thiol functionalities were incorporated into the substrates. Image obtained from Beaumont et al. (2018)

affect the dispersibility of the substrates in solvents and also their physical properties.

Beaumont et al. (2018) described a two-step general procedure for silanization of never-dried cellulose substrates. CNFs, cellulose II gel and carboxymethylated pulp were modified with silanes bearing azido, vinyl and mercapto groups, which are commonly used in click chemistry reactions. The modification was performed in aqueous medium by first hydrolyzing the alkoxysilane in the presence of catalytic amounts of HCl, followed by a condensation reaction between the formed silanols and the cellulose when NaOH is added to the reaction mixture (Fig. 13). The advantages of this reaction are that it is a water-based reaction and that it allows the attachment of many diverse functionalities to different cellulosic substrates. The reaction kinetics follow a linear zero-order model, which allows to easily control the extent of the modification. The functionalities that are grafted in this work can be used in various types of click reactions, including thiol-ene reactions and azide-alkyne cycloadditions, as well as radical polymerizations and cycloadditions in the case of vinyl-substituted substrates.

Like in the case of esterification reactions, there have been developments towards more environmentally friendly reactions within the modifications with silanes. Recently reported water-based reactions show that there is still great potential for developing the modification reactions taking into consideration the use of milder reaction conditions and avoidance of excessive use of organic solvents. Moreover, silanes can be used as a way to introduce functionalities that can undergo click chemistry reactions. Table 2 in the supplementary information (SI-Table 2) summarizes the examples mentioned in this section.

Particle deposition + silane coating

Superhydrophobicity is achieved when the water contact angle on a surface is > 150°, and is often the result of lowering the surface energy of the substrate and increasing its roughness (Samyn 2013). The most well-known superhydrophobic surfaces found in nature are lotus leaves, which are self-cleaning and have antifouling properties. Efforts have been made to mimic the surface structure of these leaves, which have nano and microstructures that can form
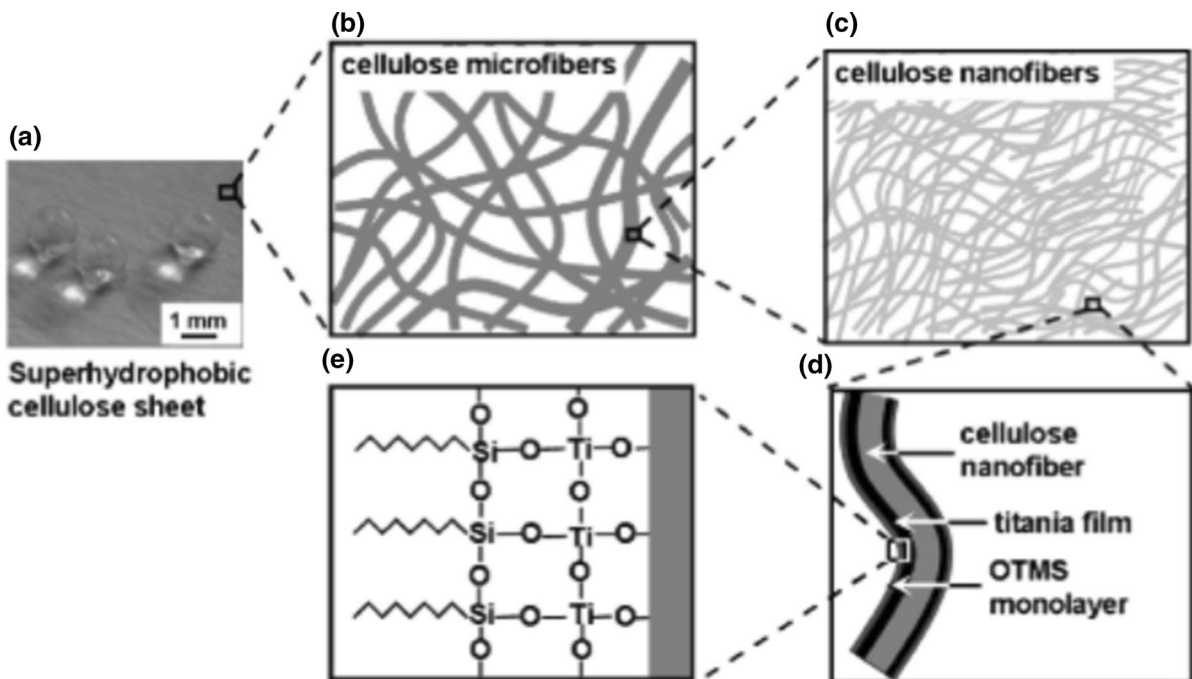
Fig. 14 Schematic representation of the modification of cellulose nanofibers by TiO$_2$ deposition and silane coating. Image obtained from Sujing et al. (2010)
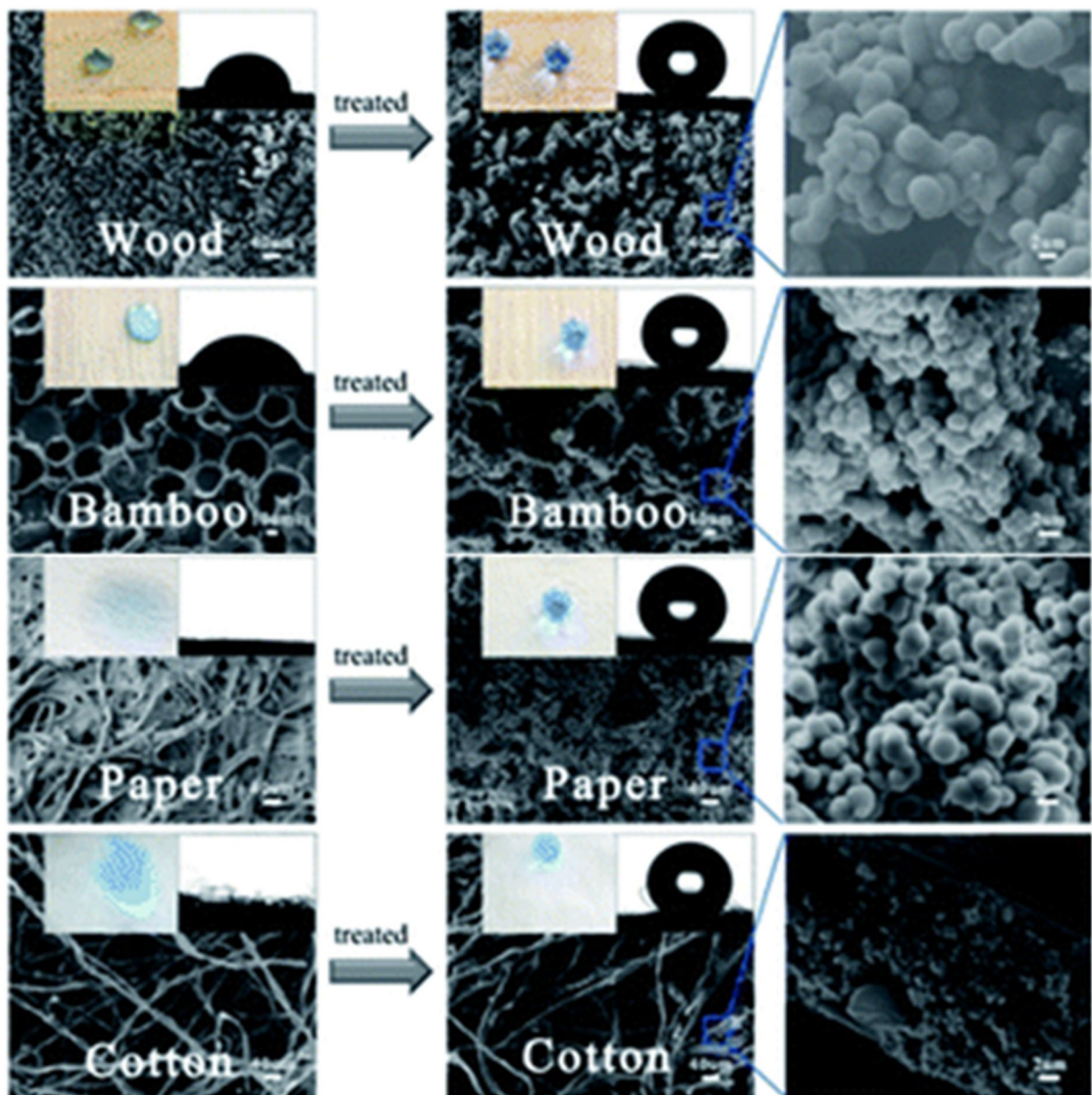
Fig. 15 Scanning electron microscope images of untreated and modified surfaces of various cellulosic materials. Image adapted from Wu et al. (2016)

air pockets, resulting in superhydrophobic properties. So far, the most common approach to obtaining superhydrophobicity on cellulosic surfaces consists of the combination of two factors: first, the deposition of particles to increase the surface roughness; and second, the coating of the substrate with a hydrophobic compound. In this section, we summarize some of the

existing methods used to obtain superhydrophobic cellulosic surfaces that follow this principle.

Cellulose fibers from filter paper were first coated with five layers of titanium oxide, and then a monolayer of octyltrimethoxysilane (OTMS) (Fig. 14) (Sujing et al. 2010). Before modification, the filter paper absorbed water droplets, but after treatment, the contact angle increased to 154.8°.

**Table 4** Overview of modifications of cellulosic materials by particle deposition followed by silane coatings

Cellulose source	Type of cellulose	Hydrophobing agent	Contact angle (°)	Ref
Filter paper	Fibers	TiO$_2$/octyltrimethoxysilane	(TiO$_2$)$_5$: 154.8 (TiO$_2$)$_{10}$: 160.5 (TiO$_2$)$_{20}$: 158.2	Sujing et al. (2010)
		TiO$_2$/(MeO)$_3$SiCH$_2$CH$_2$CH$_3$	(TiO$_2$)$_5$: 154.5 (TiO$_2$)$_{10}$: 151.9 (TiO$_2$)$_{20}$: 152.8	
		TiO$_2$/(MeO)$_3$SiCH$_2$(CH2)$_{16}$CH$_3$	(TiO$_2$)$_5$: 159.6 (TiO$_2$)$_{10}$: 151.0 (TiO$_2$)$_{20}$: 154.7	
Wood		TiO$_2$ (25 nm)/vinyltriethoxysilane	153.2	Wu et al. (2016)
Bamboo			155.1	
Paper	Fibers		153.1	
Cotton	Fibers		154.4	
Filter paper	Fibers	TiO$_2$/1H,1H,2H,2H-perfluorooctyl trimethoxysilane	154 Etched: 158	Jin et al. (2012)

The super-hydrophobic surfaces displayed very good stability since the contact angles remained unchanged even after storage in air for 18 months. The contact angles did not vary in the pH range from 3 to 11 and remained above 148° after 48 h in these solutions. Paper samples coated with 5, 10 and 20 layers of titania and a monolayer of silanes of varying chain length presented contact angles > 150°. The highest contact angle (160.5°) was obtained for paper coated with 10 layers of titania and a monolayer of OTMS.

Substrates including lignocellulosic materials such as wood, bamboo, cotton and paper were also coated with titanium oxide nanoparticles with a diameter of 25 nm, and then vinyltriethoxysilane (Fig. 15) (Wu et al. 2016). All surfaces presented contact angles above 150° for water, coffee, milk, red wine, cola, and soya sauce. The same procedure was followed to coat paper with silica nanoparticles with diameters between 15 and 100 nm, yielding contact angles above 150°. Further experiments on the effect of the size of titanium oxide particles were performed using particles with diameters between 25 and 300 nm, and showed that superhydrophobic surfaces were obtained regardless of the particle size, although the water contact angles decreased slightly with increasing particle size. The properties of all substrates remained unchanged after storage at 90% RH for 96 h.

Another technique to prepare amphiphobic surfaces consists of etching the surface of cellulose fibers in an alkaline solution, followed by deposition of five titanium oxide layers and monolayers of PFOTMS on top (Jin et al. 2012). The water and hexane contact angles of the modified surface were
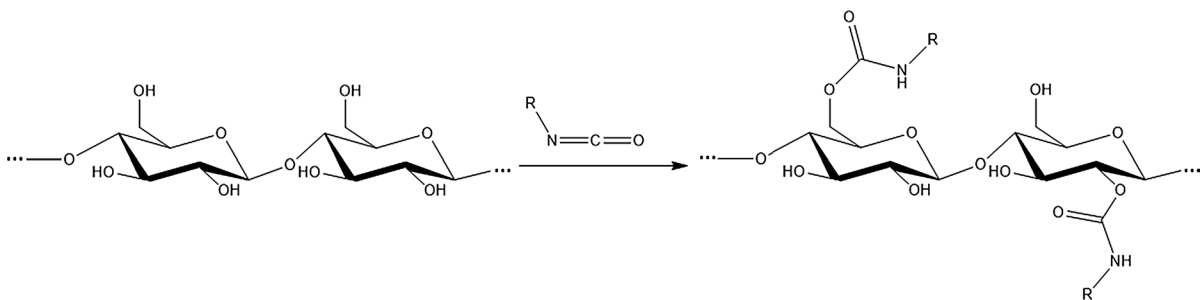
Fig. 16 Schematic representation of a carbamylation reaction

158° and 146.5°, respectively. Moreover, such surfaces presented low bacterial adhesion. Zhang et al. (2017) cross-linked CNF microspheres deposited on filter paper, followed by coating with MTMS. The diameter of the microspheres was found to be 1–10 μm. The water contact angle of the coated paper reached 162°, and the samples maintained their superhydrophobic properties while immersed in oil, allowing them to be used for oil filtration from oil/water mixtures. An overview of the methods based on particle deposition and silane coating is given in Table 4.

Carbamylation

Carbamylation of cellulose is performed by the reaction of an isocyanate with the hydroxyl groups of cellulose, resulting in the formation of a urethane moiety, as shown in Fig. 16. This type of reaction can be used to graft other types of molecules using isocyanate groups as linkers.

Surface modification

Isocyanate-terminated castor oil was used to increase the hydrophobicity of CNCs (Shang et al. 2013). The water contact angle increased from 45° to 97°. Two of the three hydroxyl groups present in castor oil were terminated with phenyl isocyanate to prevent potential cross-linking reactions. The remaining hydroxyl group was reacted with 2,4-toluene diisocyanate (TDI). The modified CNCs were dispersible in ethyl ether, toluene, acetone, DMF and THF, whereas unmodified CNCs were only dispersible in DMF and water. As pointed out in a review

by Eyley and Thielemans (2014) the authors did not take into account that castor oil is a mixture of triglycerides when calculating the extent of the modification. In another example of hydrophobization by carbamylation, cellulose fibers from Spanish Broom were extracted and hydrophobized with methylene diphenyl diisocyanate (MDI) by nebulizing this reagent on the fibers (Tursi et al. 2018). This solvent-free approach reduces the environmental impact and the cost of the experiments. The modified fibers presented a contact angle of 148° and were successfully used for the adsorption of hydrophobic organic compounds.

Modified CNCs self-assembled into layered structures were used as emulsifiers in water-in-oil (w/o) Pickering emulsions (Guo et al. 2017). The C2 and C6 hydroxyl groups of the CNCs reacted with *n*-octadecyl isocyanate, resulting in alkyl modified intercalated CNCs. The effect of the DS (0.4. 0.8. 1.8 and 1.9), reaction temperature and reaction time were investigated, allowing to adjust the wettability of the crystals to obtain the desired emulsifying properties. Only the CNCs with DS 0.8 successfully stabilized w/o emulsions. The water contact angles of modified CNC films (DS 0.8 and 1.8) were 124° and 147°, respectively, showing that increasing DS led to higher hydrophobicity.

Modification of cellulosic substrates with isocyanates has also been used as a method to graft polymers following the "grafting from" approach. Polymers such as polycaprolactone (PCL) (Habibi and Dufresne 2008), polystyrene and poly(methyl methacrylate) (Botaro and Gandini 1998) have been used to hydrophobize the substrates. This topic is discussed in more detail in (Rodríguez-Fabià et al. 2022b).
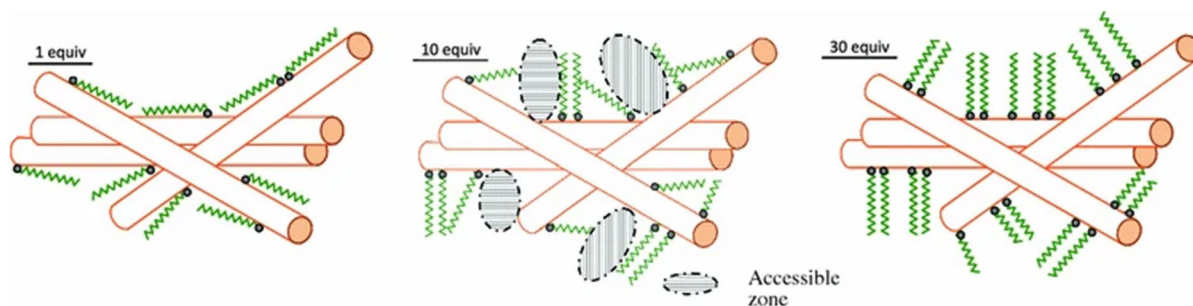
Fig. 17 Schematic representation of the grafted cellulose nanofibers at 1, 10 and 30 eq. octadecyl isocyanate. Image obtained from Missoum et al. (2012)

Bulk modification

Nanofibrillated cellulose was modified with varying concentrations of octadecyl isocyanate (1, 10 and 30 equivalents) (Missoum et al. 2012). The DS and surface DS were calculated and they both increased with increasing cyanate concentration. At low cyanate concentration, the modification only occurred at the surface. When the concentration was increased to 10 eq., both the surface and bulk of the nanofibrillated cellulose were modified. Further increase of the cyanate concentration resulted in only the modification of the surface because the high number of grafted chains hindered the diffusion of the molecules towards the bulk of the nanofibrils. The samples grafted with 10 eq. displayed contact angles of 80°,

Table 5 Overview of modifications of cellulosic materials by carbamylation. Cellulose nanocrystal (CNC), diphenyl diisocyanate (MDI), and cellulose nanofiber (CNF)

Cellulose source	Type of cellulose	Hydrophobing agent	Degree of substitution (DS)	Contact angle (°)	Ref
Surface					
Cotton linters	CNC	Castor oil-isocyanate		96.85	Shang et al. (2013)
Spanish Broom	Fibers	MDI		148	Tursi et al. (2018)
Softwood sulphite pulp	CNC	*n*-octadecyl isocyanate	0.4, 0.8, 1.8, 1.9	$DS_{0.8} = 124$ $DS_{1.8} = 147$	Guo et al. (2017)
Bulk					
Native eucalyptus fibers	CNF	*n*-octadecyl isocyanate	1 eq: 0.14* 10 eq: 0.34 30 eq: 0.47	1 eq: 90 10 eq: 80 30 eq: 90	Missoum et al. (2012)**

*Surface DS obtained from XPS

** In here the equivalents of octadecyl isocyanate are calculated with respect to the fraction of hydroxyl groups available at the surface of cellulosic nanofibers. 1 eq of octadecyl isocyanate reacts 1:1 with 1 eq of hydroxyl groups
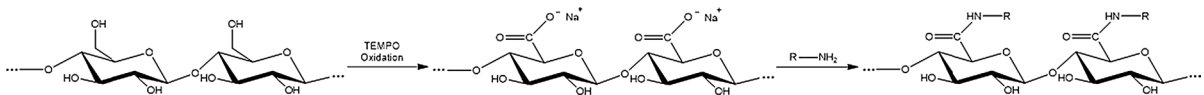
Fig. 18 Schematic representation of an amidation reaction of TEMPO-oxidized cellulose

Table 6 Overview of modifications of cellulosic materials by amidation

Cellulose source	Type of cellulose	Hydrophobing agent	Degree of substitution	Contact angle (°)	Ref
MCC	CNF	Dodecylamine	0.17	61	Gómez et al. (2017)
		Octadecylamine	0.13	67	
Date palm	CNC	*n*-propylamine	0.26	84	Bendahou et al. (2015)
		n-octylamine	0.11	92	
		Dodecylamine	0.05	86	
		Octadecylamine	0.06	94	
		Hexanoyl chloride*	0.43	92	
		Lauroyl chloride*	0.45	104	
		Stearoyl chloride*	0.36	108	

*Esterification reaction performed as a comparison

whereas samples grafted with 1 and 30 eq. had contact angles of 90°. These three different scenarios are illustrated in Fig. 17. In addition, the grafted samples presented improved resistance to thermal degradation. A summary of the modifications by carbamylation is shown in Table 5.

Amidation

Amidation of cellulosic materials usually consists of a two-step process, where the first one introduces carboxylic groups to the cellulose molecules (via esterification, TEMPO oxidation, periodate oxidation, or other methods), and the second one yields an amide bond from the reaction between these carboxylic groups and amines (Fig. 18). In the cases where TEMPO oxidation is used as a pre-treatment, the modification can only occur at the oxidized OH groups, in this case, the ones in C6. On the other hand, periodate oxidation results in the cleavage of the bond between C2 and C3, forming a dialdehyde that can form other structures (Nypelö et al. 2021).

A "one-pot" amidation reaction of TEMPO-oxidized cellulose nanofibrils (TOCNFs) was reported by Gómez et al. (2017). The reaction requires the presence of an acylating agent, in this case a uranium salt, which reacts with anionic TOCNFs, forming an active ester, which further reacts with primary amines (dodecylamine and octadecylamine). Contact angle measurements confirmed the increase in hydrophobicity after amidation. The substrates modified with dodecylamine displayed a contact angle of 61°, and the ones modified with octadecylamine of 67°, which are significantly higher than the contact angle of the unmodified TOCNFs (17°). In addition to increased hydrophobicity, the modified films also displayed improved thermal properties. Esterification and amidation of TEMPO-oxidized cellulose nanocrystals (TOCNCs) were performed using aliphatic acid chlorides and amines with chain lengths C3–C18 (Bendahou et al. 2015). The DS after esterification (0.36–0.45) was higher than after amidation (0.05–0.26). The contact angles increased with the hydrocarbon chain length and had values of 92°–108° for the esterified CNCs, and 84°–94° for the amidated ones, as shown in Table 6.

Click chemistry

Click chemistry is based on a series of orthogonal reactions that are highly selective, result in high yields and are performed in mild conditions. Typically, these reactions do not yield byproducts, or they are easily removable. Click reactions include copper(I) catalyzed azide-alkyne cycloadditions, nucleophilic ring-opening reactions, and thiol-ene reactions, among others (Hoyle and Bowman 2010).

Metal-catalyzed azide-alkyne cycloadditions are the most common click chemistry reactions. The reaction takes place between terminal alkynes and

Fig. 19 Schematic representation of metal-catalyzed azide-alkyne cycloadditions (MAAC) with copper-catalyzed azide-alkyne cycloadditions (CuAAC) as an example. Image obtained from Wang et al. (2016)
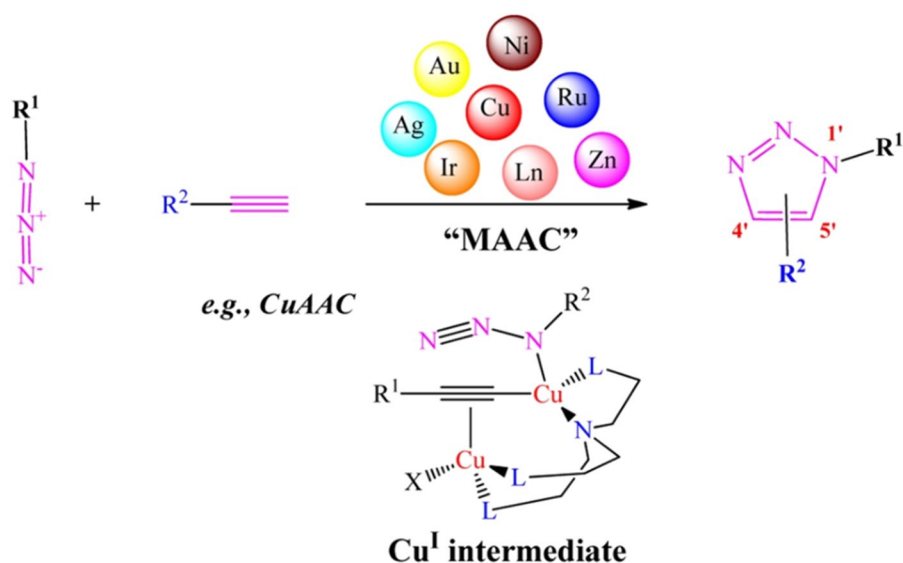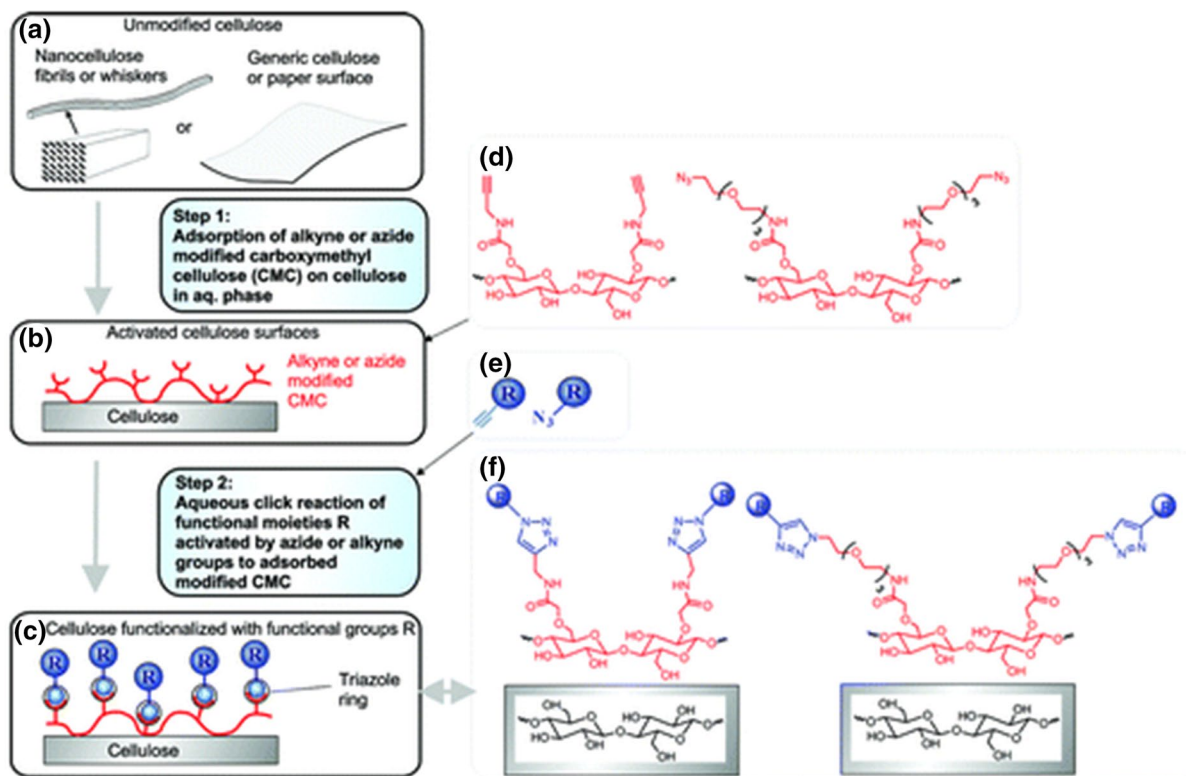
Fig. 20 Schematic representation of the modification of cellulosic materials by activation and functionalization of the surfaces. Image obtained from Filpponen et al. (2012)

azides, and Cu (I) is often used as a catalyst, although other metals (Ru, Ag, Au, Ir, Ni, Zn, Ln) can also be used (Fig. 19). The products of these reactions are 1,4-disubstituted 1,2,3-triazoles. The advantages of the copper-catalyzed reaction compared with the non-catalyzed reaction are that it is regioselective, and can be performed under milder conditions and in water or alcoholic solvents. Disubstituted alkynes cannot be used in copper-catalyzed reactions because they require deprotonation of the terminal alkyne, but it is possible to perform azide-alkyne cycloadditions with disubstituted alkynes using ruthenium (Wang et al. 2016).

A generic method for the modification of regenerated cellulose, filter paper and CNFs was developed based on azide-alkyne cycloaddition click reactions (Filpponen et al. 2012). Carboxymehtyl cellulose was functionalized with either azide or alkyne groups, and then it was adsorbed onto the different cellulosic substrates, resulting in the functionalization of these substrates, as illustrated in
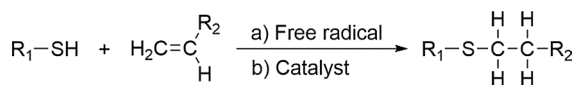
Fig. 21 Scheme of **a** a thiol-ene reaction and **b** a thiol-Michael addition where the catalyst is a base or a nucleophile

Fig. 20. The following step consisted of the click reaction between the cellulosic films and molecules with the complementary click functionalities. To demonstrate the broad applicability of this synthetic strategy, the click reaction was performed using very diverse molecules, such as a protein (bovine serum albumin), a fluorescent probe (dansyl), and a synthetic polymer (polyethylene glycol). Although hydrophobization of cellulose is not discussed in the article, this method provides the possibility of hydrophobic modification of the substrates.

Similarly, Hettegger et al. (2015, 2016) reported a method for modification of never-dried cellulosic substrates by azide-alkyne click reactions. The substrates

(BNC sheets, pulp, MFC, viscose fibers and TEN-CEL gel) were modified with (3-azidopropyl)triethoxysilane in aqueous media and at mild conditions. As a proof of concept, the azido-modified substrates were successfully reacted with an alkyne-terminated fluorescent dye through a copper-catalyzed alkylazide cycloaddition reaction. As demonstrated by the authors of this work, this is a versatile and general approach that applies to many different types of substrates and introduces azide functionalities that can easily react via click reactions with a vast number of chemical compounds.

Fatona et al. (2018) used triazine chemistry to modify the surface of CNCs, which can be used as a platform for further click-chemistry modifications. The authors modified the cyanuric chloride linker with a molecule of choice and then grafted the resulting compound onto the surface of CNCs. The substituents octadecylamine, propargylamine and benzylamine increased the hydrophobicity of the CNCs, which formed stable suspensions in chloroform. The modification did not affect the crystallinity of the CNCs. Propargylamine substituents could also be used to further graft other molecules (e.g. fluorescent dyes) by azide-alkyne click reactions. Octadecylamine was also grafted from filter paper by triazine chemistry. The reaction time increased the contact angle of the modified paper, which reached its maximum (125°) after 3 h.

Click reactions between thiols and enes can occur via a radical reaction (thiol-ene reactions) or via the formation of anionic species (thiol-Michael addition) and yield a thioether (Fig. 21). Thiol-ene reactions are usually photoinitiated. The initiator generates a thyil radical that adds to the alkene generating a carbon centred radical, which in turn abstracts a hydrogen from another thiol. On the other hand, thiol-Michael additions are base/nucleophile-catalyzed reactions that occur by nucleophilic attack of an electron-deficient C=C bond by a thiolate. The product of this reaction is an anion, which abstracts a hydrogen from another thiol or a base, forming the resulting thiolate. Both thiol-ene and thiol-Michael reactions are tolerant to the presence of air and oxygen and can be performed in various solvents, including water (Lowe 2010; Fairbanks et al. 2017).

Thiol-ene click chemistry combined with silylation was used as another approach to modify MFC films

(Tingaut et al. 2011). First, an MFC suspension was modified with either vinyltrimethoxysilane or 3-mercaptopropyltrimethoxysilane to introduce alkene and thiol functionalities, respectively. Then, films of these two qualities of MFCs were formed and further modified via a thiol-ene reaction with methylthioglycolate and allylbuyrate, respectively. A different approach consisted in clicking vinyltrimethoxysilane with methylthioglycolate, and then grafting the resulting compound onto MFC films (Fig. 22). The first and third modification pathways presented faster reaction kinetics and were more controllable than the second one. Despite not being reported in the article, these modifications introduce alkyl chains to the film surfaces, increasing the hydrophobicity of the substrates.

CNC aerogels were also modified by a thiol-ene reaction. The aerogels were first functionalized with methacrylate groups via an esterification reaction (Aalbers et al. 2019). The product was further reacted with thiols of varying hydrophobicity: 3-mercaptopropionic acid, 6-sulfonylhexan-1-ol, 1-dodecanethiol, 1H,1H,2H,2H-perfluorodecanethiol, and cysteamine. The modified aerogels were used for xylene absorption, where the most hydrophobic aerogels displayed a better performance.

Diels–Alder cycloaddition and the thiol-Michael reaction were used as a method to graft two different fluorescent dyes from CNFs based on click chemistry (Navarro et al. 2015). The first step of the modification involved modifying the CNFs with 2-furoyl chloride. Then fluorescein diacetate 5-maleimide was grafted via a Diels–Alder cycloaddition, while an additional step (a Diels–Alder cycloaddition between furoate-CNF and a bismaleimide derivative) was required before grafting 7-mercapto-4-methylcoumarin via the thiol-Michael reaction. By combining both types of click reactions, it was possible to obtain CNFs grafted with both fluorescein and coumarin resulting in multicolor labelled CNFs. This modification approach opens the possibility of simultaneously grafting different substituents based on two different click chemistry reactions.

Similarly to carbamylation, click reactions were also used to graft polymers from cellulosic substrates as a method to increase their hydrophobicity. PCL was grafted from cellulose fibers (Krouit et al. 2008), CNCs (Zhou et al. 2018), and CNFs (Pahimanolis et al. 2011) by azide-alkyne cycloaddition reactions, and from filter paper by a thiol-ene reaction (Zhao
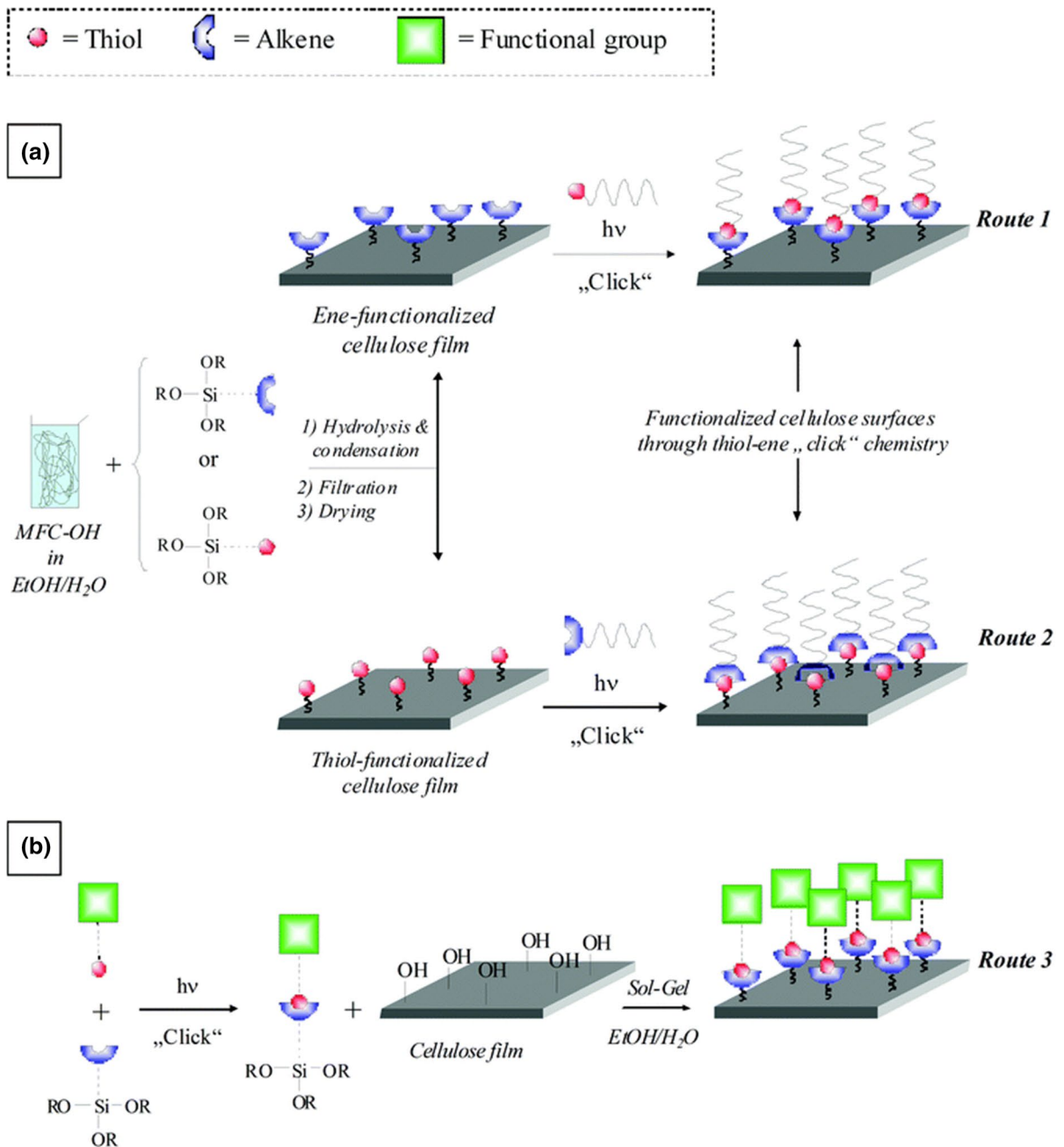
Fig. 22 Schematic representation of the three different modification pathways for cellulose surfaces using thiol-ene and silane chemistry. Image obtained from Tingaut et al. (2011)

et al. 2010). Polymer grafting is outside of the scope of this review, and therefore the topic is not discussed in detail here. A section on this topic is included in Hydrophobization of lignocellulosic materials part III:

modification with polymers (Rodríguez Fabià et al. 2022b). Table 7 summarizes the examples reported in this review based on click-chemistry reactions.

Table 7 Overview of modifications of cellulosic materials by click chemistry

Cellulose source	Type of cellulose	Type of click reaction	Hydrophobing agent	Ref
Carboxymethyl cellulose		Azide-alkyne cycloaddition	–	Filpponen et al. (2012)
BNC		Azide-alkyne cycloaddition		Hettegger et al. (2015)
Pulp, MFC, viscose fibers, TENCEL gel	Fibers, MFC	Azide-alkyne cycloaddition	–	Hettegger et al. (2016)
	CNC	Azide-alkyne cycloaddition	Propargylamine	Fatona et al. (2018)
Bleached sulphite pulp	MFC	Thiol-ene	Vinyltrimethoxysilane/methylthioglycolate, 3-mercaptopryltrimethoxysilane/allylbutyrate	Tingaut et al. (2011)
	CNC		Methacrylic anhydride/3-mercaptopropionic acid, 6-sulfonylhexan-1-ol, 1-dodecanethiol, 1H,1H,2H,2H-perfluoro-decanethiol, cysteamine	Aalbers et al. (2019)
Bleached and sulfite treated softwood pulp	CNF	Diels–Alder cycloaddition, thiol-Michael	–	Navarro et al. (2015)

Discussion

Modification at the surface or in bulk?

When modifying lignocellulosic substrates, the extent of the modification is a key parameter because in addition to, for example, increasing the hydrophobicity of the substrate, it can also modify its physical properties. The issue of the extent of the modification was also raised by Eyley and Thielemans (2014) in their review on surface modification of cellulose nanocrystals. The authors question the structural integrity of the cellulose nanocrystals (CNCs) when a surface DS larger than 1 is obtained. The authors also question the suitability of bulk techniques, such as elemental analysis, that are commonly used to estimate the surface modification of CNCs, and conclude that the crystallinity of the substrates should be analyzed before and after the modification to assess the extent of the reaction.

Although often in the literature it is not specified, it is important to differentiate between surface and bulk modification. Surface modifications are of great interest because they have minimal effects on the properties of the (nano)fibers and nanocrystals, allowing to maintain the structural and mechanical properties of these materials, as well as their molar mass (Tardy et al. 2021). Although cellulose has three hydroxyl groups available for modification, steric effects and

intrachain hydrogen bonding hinder the access to the C3-OH. Therefore, surface modifications are mostly limited to the C6-OH and the C2-OH. Recent publications (Beaumont et al. 2021a, 2021b) reported highly C6-OH regioselective acetylation reactions that limit the modification to the surface, and thus ensure the preservation of the mechanical properties of the substrates.

The significance of substrate and material composition

Based on the cited studies, utilizing nanocellulose, microfibrils, fiber or film/paper as a substrate, seemingly has no pronounced effect on the obtained DS or contact angle. The same seems to be true in terms of the crystallinity of the substrates (Table 1).

The presence of lignin and hemicellulose is poorly investigated with respect to their effect on the chemical modification of lignocellulosic substrates. A very instructive study by Castellano et al. (2004), showed that siloxanes require humidity in order to graft onto cellulose. This was due to the partial hydrolysis of siloxanes occurring only under humid conditions. However, dry modification of siloxane on lignin was feasible. This was related to the increased reactivity of the phenolic OH group in lignin as opposed to the aliphatic OH groups in cellulose. Concerning hemicellulose, the same modification routes applicable to

cellulose typically also work for hemicellulose (Fang et al. 2000; Li and Pan 2018). Several hemicellulose modification methods simply aim at modifying hydroxyl moieties as they do with cellulose. However, hemicelluloses may be partially methylated/carboxylated (Ebringerová 2005). One might then envision that other modification routes are possible.

The significance of the hydrophobization method

It is difficult to compare the results presented in this review since the substrates and the experimental methods are so diverse. However, some general trends can be observed, especially in the cases where the authors tested several modifying agents. For instance, adsorption often yields the lowest contact angles (see: Rodríguez-Fabià et al. 2022a), followed by amidation. Both etherification, esterification and carbamylation yield high contact angles, as well as silylation and particle deposition in combination with silylation. Except for surfactant adsorption, all methods are capable of yielding CAs > 90°. Superhydrophobicity (CAs > 150°) may be obtained by silylation (Table 2-SI), particle deposition + silylation (Table 4), wax adsorption, or plasma etching (see: Rodríguez-Fabià et al. 2022a). These methods often use fluorinated chemicals. However, all other referred methods except for surfactant adsorption and amidation yielded contact angle values close to the 150° threshold.

Covalent modification methods are characterized by the degree of substitution. There was no direct correlation between DS and obtained contact angle, as this also depends on the substituent type and substrate, which varied across the studies. A general observation is that for the same substrate and modification route, the contact angle usually increases with increasing chain length of the modifying agent. Esterification and silylation are the most common modification techniques for hydrophobization of cellulosic materials. These two techniques have been used both for solution and gas-phase modification, and more recently water-based reactions.

One of the most effective methods to obtain (super) hydrophobic materials is the use of fluorinated chemicals often in combination with nanoparticles. Despite providing the substrates with high hydrophobicity, fluorinated chemicals and other hydrophobing agents pose a threat to the health and the environment and

are not suitable for use in food packaging and other applications. In the case of nanoparticles, the health and environmental effects of most of these materials are still unknown. Thus, hydrophobized materials necessarily need to be rinsed before use. Furthermore, chemical leaching may occur during use. It is thus extremely important to evaluate this thoroughly. In our opinion, specific material requirements and material testing is an immature field that needs to be further developed. The complexities of this process are described by Neltner et al. (2011). Therefore, it is paramount that environmentally friendly methods for hydrophobization of celluloses are developed.

Is a hydrophobized cellulosic material waterproof?

The term waterproof is a difficult one, as water may be vapour or liquid and have various pressures and temperatures. Seemingly, one aim is to increase the use of lignocellulosic materials in food packaging materials and reduce the amount of plastic in e. g. the carton laminate composite for packaging of liquids. From a material point of view, a material becomes waterproof when:

- The material has a low enough porosity
- Is sufficiently hydrophobic.

In this paper, the references utilize different methods to demonstrate water repellency. However, by "waterproof" one typically refers to not allowing the passage of liquid water upon filtration. Typically, cellulosic materials are not waterproof, but may become so by incorporating suitable nanoparticles (Farooq et al. 2019). As of yet, hydrophobized cellulose has only limited waterproof characteristics such as high contact angle and low water vapor transmission rate (WVTR). A recent study (Tedeschi et al. 2021) claims "waterproof" cellulose reaches similar contact angles and WVTRs as nylons and Teflon but does not discuss the material interactions with liquid water.

The general focus on hydrophobization in the literature is to achieve high contact angles or improved water repellency using methods ranging from "simple" (e. g. silylation) to more advanced (e. g. advanced click chemistry). Generally, the aim is to increase contact angles of the lignocellulosic substrates from about 30° to above 90°, which is the usual contact angles for most plastics, e.g. 102° for

polyethylene (De Geyter et al. 2008), and 97° for polypropylene (Vlaeva et al. 2012); although some plastics such as polylactic acid may have contact angles slightly below 90° (Guo et al. 2015).

Though we do not criticize these efforts, we believe that the focus should be shifted towards maintaining an adequate water repellency over longer times as opposed to simply achieving high contact angles. From the referenced studies it should be clear that cellulosic materials are as of now still unsatisfactory as liquid water barrier materials.

Green perspectives in hydrophobization

The 12 principles of Green Chemistry (Anastas and Warner 1998) may be used as a guideline to evaluate the hydrophobization methods. In terms of *prevention of waste*, the E-factor of most reactions, a parameter that relates the weight of produced waste to the weight of the desired product, is typically above 500, meaning that 500 kg of waste is generated per kg product. For multi-step reactions, this number is estimated to be more than 1000 (Sheldon 2007). The atom economy becomes poorer when halogens are a by-product of substitution (Lee et al. 2020), or when pH adjustment is required (Bendahou et al. 2015). It is here worth noting that a large substituent (OTMS at 374.7 g/mol vs TCMS at 149,5 g/mol) also improves the atom economy. The use of *catalysts* is also important. Catalysts are preferred over reducing/oxidizing agents, as they improve atom economy. Implementing *less hazardous chemical synthesis* and *safer solvents and auxiliaries* is achieved by avoiding organic solvents, and hydrophobing agents that cause harmful effects on the environment. A notable study is the one-pot hydrophobization by Hu et al. (2017), performing hydrophobization of CNC in water by attaching tannic acid and decylamine. Though we note that decylamine is harmful, the entire reaction was performed in water with tannic acid and CNCs as the major constituent. However, we note that the final contact angle was below 90° (74.4°). Protocols for water-based silanization have also been developed, which yielded relatively high grafting densities, about 0.4 mmol/g (Beaumont et al. 2018). However, the water contact angle is not reported. These studies highlight the fact that the substituent supposed to render hydrophobicity, should also be mildly water-soluble if water is to be used as the solvent. In turn,

this will influence the degree of obtained hydrophobicity, since as of now, the highest contact angles are obtained in organic solvents (Bendahou et al. 2015; Orsolini et al. 2018; Tursi et al. 2018; Lee et al. 2020). Material structural modification before hydrophobization is perhaps a route that could render materials more hydrophobic without using chemicals. Orsolini et al. (2018) showed that porous materials were slightly more hydrophobic compared to dense materials after hydrophobization, most likely due to improved diffusion of the hydrophobing agent through the porous structure. Others have shown that hornification of lignocellulosic material may give contact angles above 90° by reducing hydroxyl group accessibility (Ding et al. 2019; Yang et al. 2019). Hornification without simultaneous reduction in the degree of polymerization increases material stiffness which might be problematic for some end-user applications.

Applications of hydrophobic cellulosic materials

Cellulosic materials can be used in the form of fibers, paper, films, microspheres and hydrogels. These materials have very different properties and can be employed in a wide range of applications including packaging, oil/water separation, water-repellent and self-cleaning materials, or composite materials (Dufresne 2013; Wei et al. 2020). In most cases, for example in packaging or composites, the goal for material development is to replace materials from fossil fuel sources with a more sustainable alternative.

The role of hydrophobization in packaging

As discussed in Rodríguez-Fabià et al. (2022a), water swelling is a diverse concept, that is characterized by several different methods. The aim of hydrophobization is typically to reduce swelling kinetics (e. g. the time it takes to sorb water) as well as the maximal amount sorbed. The reason for this in packaging, is that swelling deteriorates the lignocellulosic material either mechanically or by increasing gas (including water) permeation. The most problematic (ambient) gases in food preservation are water, CO_2 and oxygen. A collection of literature values of these permeabilities are found in the supplementary information.

The gas permeation values in the supplementary information (SI-Table 3) should serve as a reminder that lignocellulosic materials may have comparable or even better properties than plastics, when they have not sorbed water. The effect of material swelling was illustrated by Fukuzumi et al. (2011), where the oxygen permeability (oxygen transfer rate, OTR) of TOCNF-Na-film was investigated at 23 °C and at both 0% relative humidity (RH) and 50% RH. The corresponding OTRs were 10^{-4} and 2×10^{-2} mL $\times$ cm/($m^2 \times 24$ h $\times$ atm), indicating a 200-fold increase at 50% RH. Aulin et al. (2010) found that a water content of 15 wt%, was the threshold where water started to heavily influence oxygen permeability. Bardet et al. (2015) prepared CNF films with different nanofillers: montmorillonite (MMT) and TOCNC. After thermal treatment of the CNF/TOCNC films, the oxygen permeability of the film was similar to that of the CNF/MMT film (2.1 and 1.7 cm^3 μm m^{-2} day^{-1} kPa^{-1}, respectively) at 85% RH. These studies truly underline the effect of lignocellulosic water sorption on gas permeation and will not be detailed further. Secondly, as with gas permeation, lignocellulosic materials are sensitive to water uptake. This has been demonstrated by Aulin et al. (2010), where the carboxylated MFC film storage modulus declined from 30 to 19 GPa, at ~25 wt% swelling. A decline in both Youngs modulus and tensile strength with increasing film water content has also been found by Zhang et al. (2016).

Plastic materials have a very diverse range of pore sizes dependent on the type of polymer, chain length and film fabrication method (Elyashevich et al. 2005; Bernards and Desai 2010). In this context, pore size alone may be equal to or smaller/larger compared to cellulosic films (Guo and Catchmark 2012; Östlund et al. 2013). Gas permeabilities are thus not necessarily lower in plastic compared to cellulosic materials (SI-Table 1). This feature is of course also dependent on the cellulose/polymer chemistry, temperature and water content. In terms of water swelling/penetration, plastic materials are usually superior barrier materials. This is a question of film thickness and porosity, but also a matter of chemistry. In all the referenced studies, several hydrophilic hydroxyl groups in cellulose remain after hydrophobization, as indicated by DS < 3. Hydroxyl groups will eventually interact with water, and the subsequent water swelling increases the pore size and reduces the material density (Sjöstedt et al. 2015). In this context, it is worth noting that

the degradation of hydrophobization is not investigated in most of the referenced studies. Such degradation may in addition to making the barrier water permeable, also pose a toxicity risk for the consumer (Garnier et al. 1998). This is particularly important when considering that fluorination is a well-established hydrophobization method.

Several studies that initially reach (super)hydrophobic behaviour focus on a very short time characterization of water repellency parameters (droplet roll-off, WVTR, contact angle) (Reverdy et al. 2018). Such studies do not focus on whether the produced material is suitable for packaging. Regarding packaging, it is fair to assume that water repellency may be limited to water vapour permeability between 0 and 30 °C. Moreover, one might envision that products (liquids) may be stored long term (weeks) inside such materials. In most of the reported examples, the achieved contact angles decline over short times (minutes) and are generally not recorded over longer times (Shang et al. 2018; Yuan and Wen 2018; Huang et al. 2019). We finally note that the modified AKD impregnation (Adenekan and Hutton-Prager 2019) method gave hydrophobic surfaces after 140 days. Even though a new sample was most likely used per measurement (the droplet was not positioned continuously at the same sample area for 140 consecutive days) this shows that the AKD method is most likely superior to all other methods presented in this paper when it comes to the stability of the hydrophobic coating. Other chemical modification methods likely provide equally stable surfaces, but the data is not available. From a resource-saving perspective, it would be favorable to replace AKD methods with chemical-free (e.g. plasma) methods. However, this might not be feasible for most applications.

Oil and water separation

In the "Chemical hydrophobization techniques by molecule substitution" section, many examples of cellulose aerogels and filter paper for oil/water separation are given. Cellulose aerogels are used as oil absorbents and are typically modified by chemical vapor deposition. These materials have attracted a lot of interest due to their biodegradability, renewability, low density, high porosity and good mechanical properties. Several of the modified aerogels presented in this review demonstrated better oil sorption capacities

than commercial absorbents (Sai et al. 2015; Laitinen et al. 2017; Rafieian et al. 2018). In general, the sorption capacity increases with decreasing density of the oil. For instance, Laitinen et al. (2017) developed CNF aerogels that could absorb up to 142.9 g/g of marine diesel oil, while commercial polypropylene absorbents had a capacity of 8.1–24.6 g/g. The authors also tested other types of oils and organic solvents, and in all cases, the modified aerogels performed better than the commercial materials. One of the advantages of using cellulose-based aerogels for oil sorption is that the oil can be recovered by simple squeezing of the aerogels, which allows for the reutilization of the sorbents. A key factor in the development of these materials is their recyclability, meaning how many times they can be reused, and their sorption capacity after each cycle. Some promising results have already been obtained (Laitinen et al. 2017), where the sorption capacity is as high as 70% after 30 cycles, but in other cases the sorption capacity drops after the first cycle (Mulyadi et al. 2016). Similarly, hydrophobic filter paper can be used to separate oil/water mixtures. In this case, the oil flux through the filter and the separation efficiency are the key parameters. Yu et al. (2019) reported hydrophobic filter paper that presented a separation above 99% of heavy organic solvent/water mixtures that was maintained after 30 filtration cycles. This type of paper with both hydrophobic and lipophilic properties can be an energy-efficient alternative to the current oil/water separation methods since it does not require any energy input.

Water-repellent and self-cleaning materials

Water-repellent and self-cleaning surfaces are superhydrophobic surfaces with very low sliding angles. This allows the water droplets to slide on the surface, mimicking the lotus leaves (Wei et al. 2020). This type of cellulose material is often found in the textile industry, where superhydrophobic cotton is used for waterproof, stain-resistant, self-cleaning and anti-biofouling textiles (Teisala et al. 2014). One of the most important requirements for the textile industry is that the modification of cotton fabric must withstand abrasion and several cycles of washing (Yang et al. 2018).

Composite materials

There are many examples mentioned in this review where cellulosic materials are used as

reinforcements in composites (Habibi and Dufresne 2008; Li et al. 2019). In these cases, hydrophobization enhances the dispersibility of the cellulosic material within the matrix as well as the compatibility between the two components, often resulting in an improvement of the mechanical and physical properties of the composite. For instance, Li et al. (2019) developed a biocomposite consisting of acetylated CNCs in a PHBH matrix that improved both the tensile strength and Young's modulus by over 20% with respect to unmodified CNC/PHBH composites. Similarly, the water vapor and oxygen permeability were improved by 76 and 30% compared with the unmodified CNC/PHBH composites.

However, the applications of hydrophobic cellulosic materials are not limited to the ones mentioned above. Other fields of interest are microfluidic devices (Li et al. 2010), printed electronics (Gozutok et al. 2019), and applications closely related to the packaging industry such as printing paper, and water-repellent paper and cardboard (Wu et al. 2016). Although this review mainly focuses on the hydrophobization of CNF/CNC, in industry the hydrophobization of paper or pulp (kraft and mechanical pulp) is more relevant.

Conclusions

This review offers a comprehensive overview of the state-of-the-art of cellulose hydrophobization by chemical modifications. We believe that this subject is of great importance due to the increasing demand for sustainable, environmentally friendly materials over the last few years. Cellulosic materials have the potential to replace fossil fuel-based materials in many fields, and hydrophobization of (nano)celluloses plays a key role in this development. Recent trends in cellulose hydrophobization show not only the interest in profiting from natural fibers, but also to conceive new "greener" strategies that require fewer chemicals from fossil fuel sources and that are more energy efficient.

Declarations

Conflict of interest All the authors declare no conflicts of interest.

Ethics approval The authors confirm that there were no ethical in preparing this manuscript.

Consent to participate All authors consent to participating in this work.

Consent for publication All authors consent to publishing this work.

References

Aalbers GJW, Boott CE, D'Acierno F, Lewis L, Ho J, Michal CA, Hamad WY, MacLachlan MJ (2019) Post-modification of cellulose nanocrystal aerogels with thiol-ene click chemistry. Biomacromolecules 20(7):2779–2785. https://doi.org/10.1021/acs.biomac.9b00533

Abraham E, Kam D, Nevo Y, Slattegard R, Rivkin A, Lapidot S, Shoseyov O (2016) Highly modified cellulose nanocrystals and formation of epoxy-nanocrystalline cellulose (CNC) nanocomposites. ACS Appl Mater Interfaces 8(41):28086–28095. https://doi.org/10.1021/acsami.6b09852

Adenekan K, Hutton-Prager B (2019) Sticky hydrophobic behavior of cellulose substrates impregnated with alkyl ketene dimer (AKD) via sub- and supercritical carbon dioxide. Colloids Surf A 560:154–163. https://doi.org/10.1016/j.colsurfa.2018.09.073

Anastas PT, Warner JC (1998) Green chemistry: theory and practice. Oxford University Press, New York

Andresen M, Stenius P (2007) Water-in-oil emulsions stabilized by hydrophobized microfibrillated cellulose. J Dispers Sci Technol 28(6):837–844. https://doi.org/10.1080/01932690701341827

Andresen M, Johansson L-S, Tanem BS, Stenius P (2006) Properties and characterization of hydrophobized microfibrillated cellulose. Cellulose 13(6):665–677. https://doi.org/10.1007/s10570-006-9072-1

Andresen M, Stenstad P, Møretrø T, Langsrud S, Syverud K, Johansson L-S, Stenius P (2007) Nonleaching antimicrobial films prepared from surface-modified microfibrillated cellulose. Biomacromolecules 8(7):2149–2155. https://doi.org/10.1021/bm070304e

Arancibia F, Izquierdo E, Pereira M (2021) Stabilization of the emulsion of Alkenyl Succinic Anhydride (ASA) in water using cellulose nanofibrils. Chem Eng Sci 233:116407. https://doi.org/10.1016/j.ces.2020.116407

Ashish K, Bhardwaj NK, Singh SP (2019) Cationic starch and polyacrylamides for alkenyl succinic anhydride (ASA) emulsification for sizing of cellulosic fibers. Cellulose 26(18):9901–9915. https://doi.org/10.1007/s10570-019-02758-6

Aulin C, Gällstedt M, Lindström T (2010) Oxygen and oil barrier properties of microfibrillated cellulose films and coatings. Cellulose 17(3):559–574. https://doi.org/10.1007/s10570-009-9393-y

Ávila Ramírez JA, Gómez Hoyos C, Arroyo S, Cerrutti P, Foresti ML (2016) Acetylation of bacterial cellulose catalyzed by citric acid: use of reaction conditions for tailoring the esterification extent. Carbohydr Polym 153:686–695. https://doi.org/10.1016/j.carbpol.2016.08.009

Ávila Ramírez JA, Fortunati E, Kenny JM, Torre L, Foresti ML (2017) Simple citric acid-catalyzed surface esterification of cellulose nanocrystals. Carbohydr Polym 157:1358–1364. https://doi.org/10.1016/j.carbpol.2016.11.008

Bae JH, Kim SH (2015) Alkylation of mixed micro- and nanocellulose to improve dispersion in polylactide. Polym Int 64(6):821–827. https://doi.org/10.1002/pi.4858

Barbosa RFS, Souza AG, Ferreira FF, Rosa DS (2019) Isolation and acetylation of cellulose nanostructures with a homogeneous system. Carbohydr Polym 218:208–217. https://doi.org/10.1016/j.carbpol.2019.04.072

Bardet R, Reverdy C, Belgacem N, Leirset I, Syverud K, Bardet M, Bras J (2015) Substitution of nanoclay in high gas barrier films of cellulose nanofibrils with cellulose nanocrystals and thermal treatment. Cellulose 22(2):1227–1241. https://doi.org/10.1007/s10570-015-0547-9

Beaumont M, Bacher M, Opietnik M, Gindl-Altmutter W, Potthast A, Rosenau T (2018) A general aqueous silanization protocol to introduce vinyl, mercapto or azido functionalities onto cellulose fibers and nanocelluloses. Molecules. https://doi.org/10.3390/molecules23061427

Beaumont M, Winklehner S, Veigel S, Mundigler N, Gindl-Altmutter W, Potthast A, Rosenau T (2020) Wet

esterification of never-dried cellulose: a simple process to surface-acetylated cellulose nanofibers. Green Chem 22(17):5605–5609. https://doi.org/10.1039/D0GC02116D

Beaumont M, Jusner P, Gierlinger N, King AWT, Potthast A, Rojas OJ, Rosenau T (2021a) Unique reactivity of nanoporous cellulosic materials mediated by surface-confined water. Nat Commun 12(1):2513. https://doi.org/10.1038/s41467-021-22682-3

Beaumont M, Otoni CG, Mattos BD, Koso TV, Abidnejad R, Zhao B, Kondor A, King AWT, Rojas OJ (2021b) Regioselective and water-assisted surface esterification of never-dried cellulose: nanofibers with adjustable surface energy. Green Chem 23(18):6966–6974. https://doi.org/10.1039/D1GC02292J

Beaumont M, Tardy BL, Reyes G, Koso TV, Schaubmayr E, Jusner P, King AWT, Dagastine RR, Potthast A, Rojas OJ, Rosenau T (2021c) Assembling native elementary cellulose nanofibrils via a reversible and regioselective surface functionalization. J Am Chem Soc 143(41):17040–17046. https://doi.org/10.1021/jacs.1c06502

Bendahou A, Hajlane A, Dufresne A, Boufi S, Kaddami H (2015) Esterification and amidation for grafting long aliphatic chains on to cellulose nanocrystals: a comparative study. Res Chem Intermed 41(7):4293–4310. https://doi.org/10.1007/s11164-014-1530-z

Bernards DA, Desai TA (2010) Nanoscale porosity in polymer films: fabrication and therapeutic applications. Soft Matter 6(8):1621–1631. https://doi.org/10.1039/B922303G

Botaro VR, Gandini A (1998) Chemical modification of the surface of cellulosic fibres. 2. Introduction of alkenyl moieties via condensation reactions involving isocyanate functions. Cellulose 5(2):65–78. https://doi.org/10.1023/A:1009216729686

Castellano M, Gandini A, Fabbri P, Belgacem MN (2004) Modification of cellulose fibres with organosilanes: under what conditions does coupling occur? J Colloid Interface Sci 273(2):505–511. https://doi.org/10.1016/j.jcis.2003.09.044

Çetin NS, Tingaut P, Özmen N, Henry N, Harper D, Dadmun M, Sèbe G (2009) Acetylation of cellulose nanowhiskers with vinyl acetate under moderate conditions. Macromol Biosci 9(10):997–1003. https://doi.org/10.1002/mabi.200900073

Chadlia A, Farouk MHM (2011) Rapid homogeneous esterification of cellulose extracted from Posidonia induced by microwave irradiation. J Appl Polym Sci 119(6):3372–3381. https://doi.org/10.1002/app.32973

Cheng H, Gu B, Pennefather MP, Nguyen TX, Phan-Thien N, Duong HM (2017) Cotton aerogels and cotton-cellulose aerogels from environmental waste for oil spillage cleanup. Mater Des 130:452–458. https://doi.org/10.1016/j.matdes.2017.05.082

Chinga-Carrasco G, Kuznetsova N, Garaeva M, Leirset I, Galiullina G, Kostochko A, Syverud K (2012) Bleached and unbleached MFC nanobarriers: properties and hydrophobisation with hexamethyldisilazane. J Nanopart Res 14(12):1280. https://doi.org/10.1007/s11051-012-1280-z

Cunha AG, Gandini A (2010) Turning polysaccharides into hydrophobic materials: a critical review. Part 1. Cellulose. Cellulose 17(5):875–889. https://doi.org/10.1007/s10570-010-9434-6

Cunha AG, Freire C, Silvestre A, Neto CP, Gandini A, Belgacem MN, Chaussy D, Beneventi D (2010) Preparation of highly hydrophobic and lipophobic cellulose fibers by a straightforward gas–solid reaction. J Colloid Interface Sci 344(2):588–595. https://doi.org/10.1016/j.jcis.2009.12.057

David G, Gontard N, Guerin D, Heux L, Lecomte J, Molina-Boisseau S, Angellier-Coussy H (2019) Exploring the potential of gas-phase esterification to hydrophobize the surface of micrometric cellulose particles. Eur Polym J 115:138–146. https://doi.org/10.1016/j.eurpolymj.2019.03.042

De Geyter N, Morent R, Leys C (2008) Surface characterization of plasma-modified polyethylene by contact angle experiments and ATR-FTIR spectroscopy. Surf Interface Anal 40(3–4):608–611. https://doi.org/10.1002/sia.2611

de Menezes AJ, Pasquini D, Curvelo AADS, Gandini A (2009) Self-reinforced composites obtained by the partial oxypropylation of cellulose fibers. 1. Characterization of the materials obtained with different types of fibers. Carbohydr Polym 76(3):437–442. https://doi.org/10.1016/j.carbpol.2008.11.006

Ding Q, Zeng J, Wang B, Tang D, Chen K, Gao W (2019) Effect of nanocellulose fiber hornification on water fraction characteristics and hydroxyl accessibility during dehydration. Carbohydr Polym 207:44–51. https://doi.org/10.1016/j.carbpol.2018.11.075

Downey WF (1953) Higher alkyl ketene dimer emulsion, Google Patents

Dufresne A (2013) Nanocellulose: from nature to high performance tailored materials. De Gruyter, Berlin

Ebringerová A (2005) Structural diversity and application potential of hemicelluloses. Macromol Symp 232(1):1–12. https://doi.org/10.1002/masy.200551401

Edgar K (2004) Cellulose esters, organic. In: Mark HF (ed) Encyclopedia of polymer science and technology, 4th edn. Wiley, New York, pp 129–158

Elyashevich GK, Olifirenko AS, Pimenov AV (2005) Micro- and nanofiltration membranes on the base of porous polyethylene films. Desalination 184(1):273–279. https://doi.org/10.1016/j.desal.2005.03.055

Eyley S, Thielemans W (2014) Surface modification of cellulose nanocrystals. Nanoscale 6(14):7764–7779. https://doi.org/10.1039/C4NR01756K

Fadeev AY, McCarthy TJ (2000) Self-Assembly is not the only reaction possible between alkyltrichlorosilanes and surfaces: monomolecular and oligomeric covalently attached layers of dichloro- and trichloroalkylsilanes on silicon. Langmuir 16(18):7268–7274. https://doi.org/10.1021/la000471z

Fairbanks BD, Love DM, Bowman CN (2017) Efficient polymer–polymer conjugation via thiol-ene click reaction. Macromol Chem Phys 218(18):1700073. https://doi.org/10.1002/macp.201700073

Fang JM, Sun RC, Tomkinson J, Fowler P (2000) Acetylation of wheat straw hemicellulose B in a new non-aqueous

swelling system. Carbohydr Polym 41(4):379–387. https://doi.org/10.1016/S0144-8617(99)00102-2

Farooq M, Zou T, Riviere G, Sipponen MH, Österberg M (2019) Strong, ductile, and waterproof cellulose nanofibril composite films with colloidal lignin particles. Biomacromolecules 20(2):693–704. https://doi.org/10.1021/acs.biomac.8b01364

Fatona A, Berry RM, Brook MA, Moran-Mirabal JM (2018) Versatile surface modification of cellulose fibers and cellulose nanocrystals through modular triazinyl chemistry. Chem Mater 30(7):2424–2435. https://doi.org/10.1021/acs.chemmater.8b00511

Feng J, Nguyen ST, Fan Z, Duong HM (2015) Advanced fabrication and oil absorption properties of super-hydrophobic recycled cellulose aerogels. Chem Eng J 270:168–175. https://doi.org/10.1016/j.cej.2015.02.034

Filpponen I, Kontturi E, Nummelin S, Rosilo H, Kolehmainen E, Ikkala O, Laine J (2012) Generic method for modular surface modification of cellulosic materials in aqueous medium by sequential "click" reaction and adsorption. Biomacromolecules 13(3):736–742. https://doi.org/10.1021/bm201661k

Fox SC, Li B, Xu D, Edgar KJ (2011) Regioselective esterification and etherification of cellulose: a review. Biomacromolecules 12(6):1956–1972. https://doi.org/10.1021/bm200260d

Fukuzumi H, Saito T, Iwamoto S, Kumamoto Y, Ohdaira T, Suzuki R, Isogai A (2011) Pore size determination of TEMPO-oxidized cellulose nanofibril films by positron annihilation lifetime spectroscopy. Biomacromolecules 12(11):4057–4062. https://doi.org/10.1021/bm201079n

Fumagalli M, Ouhab D, Boisseau SM, Heux L (2013a) Versatile gas-phase reactions for surface to bulk esterification of cellulose microfibrils aerogels. Biomacromolecules 14(9):3246–3255. https://doi.org/10.1021/bm400864z

Fumagalli M, Sanchez F, Boisseau SM, Heux L (2013b) Gas-phase esterification of cellulose nanocrystal aerogels for colloidal dispersion in apolar solvents. Soft Matter 9(47):11309–11317. https://doi.org/10.1039/C3SM52062E

Fumagalli M, Sanchez F, Molina-Boisseau S, Heux L (2015) Surface-restricted modification of nanocellulose aerogels in gas-phase esterification by di-functional fatty acid reagents. Cellulose 22(3):1451–1457. https://doi.org/10.1007/s10570-015-0585-3

Garnier G, Wright J, Godbout L, Yu L (1998) Wetting mechanism of alkyl ketene dimers on cellulose films. Colloids Surf A 145(1):153–165. https://doi.org/10.1016/S0927-7757(98)00668-2

Geissler A, Chen L, Zhang K, Bonaccurso E, Biesalski M (2013) Superhydrophobic surfaces fabricated from nano- and microstructured cellulose stearoyl esters. Chem Commun 49(43):4962–4964. https://doi.org/10.1039/C3CC41568F

Gómez FN, Combariza MY, Blanco-Tirado C (2017) Facile cellulose nanofibrils amidation using a 'one-pot' approach. Cellulose 24(2):717–730. https://doi.org/10.1007/s10570-016-1174-9

Goussé C, Chanzy H, Cerrada ML, Fleury E (2004) Surface silylation of cellulose microfibrils: preparation and rheological properties. Polymer 45(5):1569–1575. https://doi.org/10.1016/j.polymer.2003.12.028

Gozutok Z, Kinj O, Torun I, Ozdemir AT, Onses MS (2019) One-step deposition of hydrophobic coatings on paper for printed-electronics applications. Cellulose 26(5):3503–3512. https://doi.org/10.1007/s10570-019-02326-y

Guo J, Catchmark JM (2012) Surface area and porosity of acid hydrolyzed cellulose nanowhiskers and cellulose produced by *Gluconacetobacter xylinus*. Carbohydr Polym 87(2):1026–1037. https://doi.org/10.1016/j.carbpol.2011.07.060

Guo C, Xiang M, Dong Y (2015) Surface modification of poly (lactic acid) with an improved alkali-acid hydrolysis method. Mater Lett 140:144–147. https://doi.org/10.1016/j.matlet.2014.10.099

Guo J, Du W, Gao Y, Cao Y, Yin Y (2017) Cellulose nanocrystals as water-in-oil pickering emulsifiers via intercalative modification. Colloids Surf A 529:634–642. https://doi.org/10.1016/j.colsurfa.2017.06.056

Habibi Y (2014) Key advances in the chemical modification of nanocelluloses. Chem Soc Rev 43(5):1519–1542. https://doi.org/10.1039/C3CS60204D

Habibi Y, Dufresne A (2008) Highly filled bionanocomposites from functionalized polysaccharide nanocrystals. Biomacromolecules 9(7):1974–1980. https://doi.org/10.1021/bm8001717

Heinze T, El Seoud OA, Koschella A (2018) Etherification of cellulose. In: Heinze T, El Seoud OA, Koschella A (eds) Cellulose derivatives: synthesis, structure, and properties. Springer, Cham, pp 429–477

Hettegger H, Sumerskii I, Sortino S, Potthast A, Rosenau T (2015) Silane meets click chemistry: towards the functionalization of wet bacterial cellulose Sheets. ChemSusChem 8(4):680–687. https://doi.org/10.1002/cssc.201402991

Hettegger H, Beaumont M, Potthast A, Rosenau T (2016) Aqueous modification of nano- and microfibrillar cellulose with a click synthon. Chemsuschem 9(1):75–79. https://doi.org/10.1002/cssc.201501358

Hoyle CE, Bowman CN (2010) Thiol-ene click chemistry. Angew Chem Int Ed 49(9):1540–1573. https://doi.org/10.1002/anie.200903924

Hu Z, Berry RM, Pelton R, Cranston ED (2017) One-pot water-based hydrophobic surface modification of cellulose nanocrystals using plant polyphenols. ACS Sustain Chem Eng 5(6):5018–5026. https://doi.org/10.1021/acssuschemeng.7b00415

Huang P, Wu M, Kuga S, Wang D, Wu D, Huang Y (2012) One-step dispersion of cellulose nanofibers by mechanochemical esterification in an organic solvent. Chemsuschem 5(12):2319–2322. https://doi.org/10.1002/cssc.201200492

Huang T, Chen C, Li D, Ek M (2019) Hydrophobic and antibacterial textile fibres prepared by covalently attaching betulin to cellulose. Cellulose 26(1):665–677. https://doi.org/10.1007/s10570-019-02265-8

Jandura P, Kokta BV, Riedl B (2000) Fibrous long-chain organic acid cellulose esters and their characterization by diffuse reflectance FTIR spectroscopy, solid-state CP/MAS 13C-NMR, and X-ray diffraction. J Appl Polym Sci 78(7):1354–1365. https://doi.org/10.1002/

1097-4628(20001114)78:7%3c1354::Aid-app60%3e3.0.Co;2-v

Jantas R, Górna K (2006) Antibacterial finishing of cotton fabrics. Fibres Text East Eur 14(1):88

Jarrah K, Hisaindee S, Al-Sayah MH (2018) Preparation of oil sorbents by solvent-free grafting of cellulose cotton fibers. Cellulose 25(7):4093–4106. https://doi.org/10.1007/s10570-018-1846-8

Jin H, Kettunen M, Laiho A, Pynnönen H, Paltakari J, Marmur A, Ikkala O, Ras RHA (2011) Superhydrophobic and superoleophobic nanocellulose aerogel membranes as bioinspired cargo carriers on water and oil. Langmuir 27(5):1930–1934. https://doi.org/10.1021/la103877r

Jin C, Jiang Y, Niu T, Huang J (2012) Cellulose-based material with amphiphobicity to inhibit bacterial adhesion by surface modification. J Mater Chem 22(25):12562–12567. https://doi.org/10.1039/C2JM31750H

Jonoobi M, Harun J, Mathew AP, Hussein MZB, Oksman K (2010) Preparation of cellulose nanofibers with hydrophobic surface characteristics. Cellulose 17(2):299–307. https://doi.org/10.1007/s10570-009-9387-9

Kargarzadeh H, Mariano M, Gopakumar D, Ahmad I, Thomas S, Dufresne A, Huang J, Lin N (2018) Advances in cellulose nanomaterials. Cellulose 25(4):2151–2189. https://doi.org/10.1007/s10570-018-1723-5

Kono H, Uno T, Tsujisaki H, Anai H, Kishimoto R, Matsushima T, Tajima K (2020) Nanofibrillated bacterial cellulose surface modified with methyltrimethoxysilane for fiber-reinforced composites. ACS Appl Nano Mater 3(8):8232–8241. https://doi.org/10.1021/acsanm.0c01670

Krouit M, Bras J, Belgacem MN (2008) Cellulose surface grafting with polycaprolactone by heterogeneous click-chemistry. Eur Polym J 44(12):4074–4081. https://doi.org/10.1016/j.eurpolymj.2008.09.016

Lackinger E, Hettegger H, Schwaiger L, Zweckmair T, Sartori J, Potthast A, Rosenau T (2016) Novel paper sizing agents based on renewables. Part 8: on the binding behavior of reactive sizing agents—the question of covalent versus adsorptive binding. Cellulose 23(1):823–836. https://doi.org/10.1007/s10570-015-0794-9

Laitinen O, Suopajärvi T, Österberg M, Liimatainen H (2017) Hydrophobic, superabsorbing aerogels from choline chloride-based deep eutectic solvent pretreated and silylated cellulose nanofibrils for selective oil removal. ACS Appl Mater Interfaces 9(29):25029–25037. https://doi.org/10.1021/acsami.7b06304

Lazzari LK, Zampieri VB, Zanini M, Zattera AJ, Baldasso C (2017) Sorption capacity of hydrophobic cellulose cryogels silanized by two different methods. Cellulose 24(8):3421–3431. https://doi.org/10.1007/s10570-017-1349-z

Lee K-Y, Quero F, Blaker JJ, Hill CAS, Eichhorn SJ, Bismarck A (2011) Surface only modification of bacterial cellulose nanofibres with organic acids. Cellulose 18(3):595–605. https://doi.org/10.1007/s10570-011-9525-z

Lee JH, Park SH, Kim SH (2020) Surface alkylation of cellulose nanocrystals to enhance their compatibility with polylactide. Polymers 12(1):178

Li L, Neivandt DJ (2019) The mechanism of alkyl ketene dimer (AKD) sizing on cellulose model films studied by sum frequency generation vibrational spectroscopy. Cellulose 26(5):3415–3435. https://doi.org/10.1007/s10570-019-02295-2

Li Z, Pan X (2018) Strategies to modify physicochemical properties of hemicelluloses from biorefinery and paper industry for packaging material. Rev Environ Sci Biotechnol 17(1):47–69. https://doi.org/10.1007/s11157-018-9460-7

Li X, Tian J, Garnier G, Shen W (2010) Fabrication of paper-based microfluidic sensors by printing. Colloids Surf B 76(2):564–570. https://doi.org/10.1016/j.colsurfb.2009.12.023

Li M-F, Sun S-N, Xu F, Sun R-C (2011) Cold NaOH/urea aqueous dissolved cellulose for benzylation: synthesis and characterization. Eur Polym J 47(9):1817–1826. https://doi.org/10.1016/j.eurpolymj.2011.06.013

Li D, Zhou J, Ma X, Li J (2019) Synthesis of a novel biocomposite of poly (3-hydroxybutyrate-co-3-hydroxyhexanoate) reinforced with acetylated cellulose nanocrystals. Cellulose 26(16):8729–8743. https://doi.org/10.1007/s10570-019-02708-2

Lindfors J, Salmi J, Laine J, Stenius P (2007) AKD and ASA model surfaces: preparation and characterization. BioResources 2(4):2007

Lindström T, Larsson PT (2008) Alkyl ketene dimer (AKD) sizing—a review. Nord Pulp Pap Res J 23(2):202–209

Lowe AB (2010) Thiol-ene "click" reactions and recent applications in polymer and materials synthesis. Polym Chem 1(1):17–36. https://doi.org/10.1039/B9PY00216B

Ly B, Belgacem MN, Bras J, Brochier Salon MC (2010) Grafting of cellulose by fluorine-bearing silane coupling agents. Mater Sci Eng C 30(3):343–347. https://doi.org/10.1016/j.msec.2009.11.009

Missoum K, Bras J, Belgacem MN (2012) Organization of aliphatic chains grafted on nanofibrillated cellulose and influence on final properties. Cellulose 19(6):1957–1973. https://doi.org/10.1007/s10570-012-9780-7

Missoum K, Belgacem MN, Bras J (2013) Nanofibrillated cellulose surface modification: a review. Materials 6(5):1745–1766

Müller Y, Tot I, Potthast A, Rosenau T, Zimmermann R, Eichhorn K-J, Nitschke C, Scherr G, Freudenberg U, Werner C (2010) The impact of esterification reactions on physical properties of cellulose thin films. Soft Matter 6(15):3680–3684. https://doi.org/10.1039/C0SM00005A

Mulyadi A, Zhang Z, Deng Y (2016) Fluorine-free oil absorbents made from cellulose nanofibril aerogels. ACS Appl Mater Interfaces 8(4):2732–2740. https://doi.org/10.1021/acsami.5b10985

Navarro JRG, Conzatti G, Yu Y, Fall AB, Mathew R, Edén M, Bergström L (2015) Multicolor fluorescent labeling of cellulose nanofibrils by click chemistry. Biomacromolecules 16(4):1293–1300. https://doi.org/10.1021/acs.biomac.5b00083

Neltner TG, Kulkarni NR, Alger HM, Maffini MV, Bongard ED, Fortin ND, Olson ED (2011) Navigating the U.S. food additive regulatory program. Comp Rev Food Sci Food Saf 10(6):342–368. https://doi.org/10.1111/j.1541-4337.2011.00166.x

Nypelö T, Berke B, Spirk S, Sirviö JA (2021) Review: periodate oxidation of wood polysaccharides—modulation of

hierarchies. Carbohydr Polym 252:117105. https://doi.org/10.1016/j.carbpol.2020.117105

Orsolini P, Antonini C, Stojanovic A, Malfait WJ, Caseri WR, Zimmermann T (2018) Superhydrophobicity of nanofibrillated cellulose materials through polysiloxane nanofilaments. Cellulose 25(2):1127–1146. https://doi.org/10.1007/s10570-017-1636-8

Östlund Å, Idström A, Olsson C, Larsson PT, Nordstierna L (2013) Modification of crystallinity and pore size distribution in coagulated cellulose films. Cellulose 20(4):1657–1667. https://doi.org/10.1007/s10570-013-9982-7

Pahimanolis N, Hippi U, Johansson L-S, Saarinen T, Houbenov N, Ruokolainen J, Seppälä J (2011) Surface functionalization of nanofibrillated cellulose using click-chemistry approach in aqueous media. Cellulose 18(5):1201. https://doi.org/10.1007/s10570-011-9573-4

Park S, Baker JO, Himmel ME, Parilla PA, Johnson DK (2010) Cellulose crystallinity index: measurement techniques and their impact on interpreting cellulase performance. Biotechnol Biofuels 3(1):10. https://doi.org/10.1186/1754-6834-3-10

Pasquini D, Belgacem MN, Gandini A, Curvelo AADS (2006) Surface esterification of cellulose fibers: characterization by DRIFT and contact angle measurements. J Colloid Interface Sci 295(1):79–83. https://doi.org/10.1016/j.jcis.2005.07.074

Paulsson M, Sirnonson R, Westerrnark U (1994) Chemical modification of lignin-rich paper: Part 1. Acetylation of paper made from spruce TMP and aspen CTMP. Evaluation of paper properties. Nord Pulp Pap Res J 9(4):232–236. https://doi.org/10.3183/npprj-1994-09-04-p232-236

Peresin MS, Kammiovirta K, Heikkinen H, Johansson L-S, Vartiainen J, Setälä H, Österberg M, Tammelin T (2017) Understanding the mechanisms of oxygen diffusion through surface functionalized nanocellulose films. Carbohydr Polym 174:309–317. https://doi.org/10.1016/j.carbpol.2017.06.066

Rafieian F, Hosseini M, Jonoobi M, Yu Q (2018) Development of hydrophobic nanocellulose-based aerogel via chemical vapor deposition for oil separation for water treatment. Cellulose 25(8):4695–4710. https://doi.org/10.1007/s10570-018-1867-3

Rao X, Kuga S, Wu M, Huang Y (2015) Influence of solvent polarity on surface-fluorination of cellulose nanofiber by ball milling. Cellulose 22(4):2341–2348. https://doi.org/10.1007/s10570-015-0659-2

Reverdy C, Belgacem N, Moghaddam MS, Sundin M, Swerin A, Bras J (2018) One-step superhydrophobic coating using hydrophobized cellulose nanofibrils. Colloids Surf A 544:152–158. https://doi.org/10.1016/j.colsurfa.2017.12.059

Ritchie H, Rose M (2018) Plastic pollution. https://ourworldindata.org/plastic-pollution. Retrieved 04.02.2021

Rodionova G, Hoff B, Lenes M, Eriksen Ø, Gregersen Ø (2013) Gas-phase esterification of microfibrillated cellulose (MFC) films. Cellulose 20(3):1167–1174. https://doi.org/10.1007/s10570-013-9887-5

Rodríguez-Fabià S, Torstensen J, Johansson L, Syverud K (2022a) Hydrophobisation of lignocellulosic materials part I: physical modification. Cellulose. https://doi.org/10.1007/s10570-022-04620-8

Rodríguez-Fabià S, Torstensen J, Johansson L, Syverud K (2022b) Hydrophobization of lignocellulosic materials part III: modification with polymers. Cellulose 29(11):5943–5977. https://doi.org/10.1007/s10570-022-04660-0

Russler A, Wieland M, Bacher M, Henniges U, Miethe P, Liebner F, Potthast A, Rosenau T (2012) AKD-Modification of bacterial cellulose aerogels in supercritical CO2. Cellulose 19(4):1337–1349. https://doi.org/10.1007/s10570-012-9728-y

Sai H, Fu R, Xing L, Xiang J, Li Z, Li F, Zhang T (2015) Surface modification of bacterial cellulose aerogels' web-like skeleton for oil/water separation. ACS Appl Mater Interfaces 7(13):7373–7381. https://doi.org/10.1021/acsami.5b00846

Samyn P (2013) Wetting and hydrophobic modification of cellulose surfaces for paper applications. J Mater Sci 48(19):6455–6498. https://doi.org/10.1007/s10853-013-7519-y

Sassi J-F, Chanzy H (1995) Ultrastructural aspects of the acetylation of cellulose. Cellulose 2(2):111–127. https://doi.org/10.1007/BF00816384

Schenker U, Chardot J, Missoum K, Vishtal A, Bras J (2021) Short communication on the role of cellulosic fiber-based packaging in reduction of climate change impacts. Carbohydr Polym 254:117248. https://doi.org/10.1016/j.carbpol.2020.117248

Sehaqui H, Kulasinski K, Pfenninger N, Zimmermann T, Tingaut P (2017) Highly carboxylated cellulose nanofibers via succinic anhydride esterification of wheat fibers and facile mechanical disintegration. Biomacromolecules 18(1):242–248. https://doi.org/10.1021/acs.biomac.6b01548

Shang W, Huang J, Luo H, Chang PR, Feng J, Xie G (2013) Hydrophobic modification of cellulose nanocrystal via covalently grafting of castor oil. Cellulose 20(1):179–190. https://doi.org/10.1007/s10570-012-9795-0

Shang Q, Liu C, Hu Y, Jia P, Hu L, Zhou Y (2018) Bio-inspired hydrophobic modification of cellulose nanocrystals with castor oil. Carbohydr Polym 191:168–175. https://doi.org/10.1016/j.carbpol.2018.03.012

Sheldon RA (2007) The E factor: fifteen years on. Green Chem 9(12):1273–1283. https://doi.org/10.1039/B713736M

Shimizu Y-i, Hayashi J (1988) A new method for cellulose acetylation with acetic acid. Sen'i Gakkaishi 44(9):451–456. https://doi.org/10.2115/fiber.44.9_451

Sjöstedt A, Wohlert J, Larsson PT, Wågberg L (2015) Structural changes during swelling of highly charged cellulose fibres. Cellulose 22(5):2943–2953. https://doi.org/10.1007/s10570-015-0701-4

Sujing L, Yunqian W, Jianguo H (2010) Facile fabrication of superhydrophobic cellulose materials by a nanocoating approach. Chem Lett 39(1):20–21. https://doi.org/10.1246/cl.2010.20

Tang Z, Li H, Hess DW, Breedveld V (2016) Effect of chain length on the wetting properties of alkyltrichlorosilane coated cellulose-based paper. Cellulose 23(2):1401–1413. https://doi.org/10.1007/s10570-016-0877-2

Tardy BL, Mattos BD, Otoni CG, Beaumont M, Majoinen J, Kämäräinen T, Rojas OJ (2021) Deconstruction and reassembly of renewable polymers and biocolloids into next generation structured materials. Chem Rev 121(22):14088–14188. https://doi.org/10.1021/acs.chemrev.0c01333

Tedeschi G, Guzman-Puyol S, Ceseracciu L, Benitez JJ, Goldoni L, Koschella A, Heinze T, Cavallo G, Dichiarante V, Terraneo G, Athanassiou A, Metrangolo P, Heredia-Guerrero JA (2021) Waterproof-breathable films from multi-branched fluorinated cellulose esters. Carbohydr Polym 271:118031. https://doi.org/10.1016/j.carbpol.2021.118031

Teisala H, Tuominen M, Kuusipalo J (2014) Superhydrophobic coatings on cellulose-based materials: fabrication, properties, and applications. Adv Mater Interfaces 1(1):1300026. https://doi.org/10.1002/admi.201300026

Tingaut P, Hauert R, Zimmermann T (2011) Highly efficient and straightforward functionalization of cellulose films with thiol-ene click chemistry. J Mater Chem 21(40):16066–16076. https://doi.org/10.1039/C1JM11620G

Tomé LC, Freire MG, Rebelo LPN, Silvestre AJD, Neto CP, Marrucho IM, Freire CSR (2011) Surface hydrophobization of bacterial and vegetable cellulose fibers using ionic liquids as solvent media and catalysts. Green Chem 13(9):2464–2470. https://doi.org/10.1039/C1GC15432J

Tripathi A, Ago M, Khan SA, Rojas OJ (2018) Heterogeneous acetylation of plant fibers into micro- and nanocelluloses for the synthesis of highly stretchable, tough, and water-resistant co-continuous filaments via wet-spinning. ACS Appl Mater Interfaces 10(51):44776–44786. https://doi.org/10.1021/acsami.8b17790

Tursi A, Beneduci A, Chidichimo F, De Vietro N, Chidichimo G (2018) Remediation of hydrocarbons polluted water by hydrophobic functionalized cellulose. Chemosphere 201:530–539. https://doi.org/10.1016/j.chemosphere.2018.03.044

Vlaeva I, Yovcheva T, Viraneva A, Kitova S, Exner G, Guzhova A, Galikhanov M (2012) Contact angle analysis of corona treated polypropylene films. J Phys: Conf Ser 398:012054. https://doi.org/10.1088/1742-6596/398/1/012054

Wang C, Ikhlef D, Kahlal S, Saillard J-Y, Astruc D (2016) Metal-catalyzed azide-alkyne "click" reactions: mechanistic overview and recent trends. Coord Chem Rev 316:1–20. https://doi.org/10.1016/j.ccr.2016.02.010

Wang Y, Wang X, Xie Y, Zhang K (2018) Functional nanomaterials through esterification of cellulose: a review of chemistry and application. Cellulose 25(7):3703–3731. https://doi.org/10.1007/s10570-018-1830-3

Wei L, Agarwal UP, Hirth KC, Matuana LM, Sabo RC, Stark NM (2017) Chemical modification of nanocellulose with canola oil fatty acid methyl ester. Carbohydr Polym 169:108–116. https://doi.org/10.1016/j.carbpol.2017.04.008

Wei DW, Wei H, Gauthier AC, Song J, Jin Y, Xiao H (2020) Superhydrophobic modification of cellulose and cotton textiles: methodologies and applications. J Bioresour Bioprod 5(1):1–15. https://doi.org/10.1016/j.jobab.2020.03.001

Wen X, Wang H, Wei Y, Wang X, Liu C (2017) Preparation and characterization of cellulose laurate ester by catalyzed transesterification. Carbohydr Polym 168:247–254. https://doi.org/10.1016/j.carbpol.2017.03.074

Wu Y, Jia S, Qing Y, Luo S, Liu M (2016) A versatile and efficient method to fabricate durable superhydrophobic surfaces on wood, lignocellulosic fiber, glass, and metal substrates. J Mater Chem A 4(37):14111–14121. https://doi.org/10.1039/C6TA05259B

Wu Z, Xu J, Gong J, Li J, Mo L (2018) Preparation, characterization and acetylation of cellulose nanocrystal allomorphs. Cellulose 25(9):4905–4918. https://doi.org/10.1007/s10570-018-1937-6

Xu J, Wu Z, Wu Q, Kuang Y (2020) Acetylated cellulose nanocrystals with high-crystallinity obtained by one-step reaction from the traditional acetylation of cellulose. Carbohydr Polym 229:115553. https://doi.org/10.1016/j.carbpol.2019.115553

Yang J, Pu Y, Miao D, Ning X (2018) Fabrication of durably superhydrophobic cotton fabrics by atmospheric pressure plasma treatment with a siloxane precursor. Polymers 10(4):460

Yang W, Gao Y, Zuo C, Deng Y, Dai H (2019) Thermally-induced cellulose nanofibril films with near-complete ultraviolet-blocking and improved water resistance. Carbohydr Polym 223:115050. https://doi.org/10.1016/j.carbpol.2019.115050

Yu L, Zhang Z, Tang H, Zhou J (2019) Fabrication of hydrophobic cellulosic materials via gas–solid silylation reaction for oil/water separation. Cellulose 26(6):4021–4037. https://doi.org/10.1007/s10570-019-02355-7

Yuan Z, Wen Y (2018) Enhancement of hydrophobicity of nanofibrillated cellulose through grafting of alkyl ketene dimer. Cellulose 25(12):6863–6871. https://doi.org/10.1007/s10570-018-2048-0

Yuan H, Nishiyama Y, Kuga S (2005) Surface esterification of cellulose by vapor-phase treatmentwith trifluoroacetic anhydride. Cellulose 12(5):543–549. https://doi.org/10.1007/s10570-005-7136-2

Zhang Z, Sèbe G, Rentsch D, Zimmermann T, Tingaut P (2014) Ultralightweight and flexible silylated nanocellulose sponges for the selective removal of oil from water. Chem Mater 26(8):2659–2668. https://doi.org/10.1021/cm5004164

Zhang Z, Tingaut P, Rentsch D, Zimmermann T, Sèbe G (2015) Controlled silylation of nanofibrillated cellulose in water: reinforcement of a model polydimethylsiloxane network. Chemsuschem 8(16):2681–2690. https://doi.org/10.1002/cssc.201500525

Zhang X, Yu Y, Jiang Z, Wang H (2016) Influence of thickness and moisture content on the mechanical properties of microfibrillated cellulose (MFC) films. Wood Res 61(6):851–860

Zhang F, Ren H, Shen L, Tong G, Deng Y (2017) Micro–nano structural engineering of filter paper surface for high selective oil–water separation. Cellulose 24(7):2913–2924. https://doi.org/10.1007/s10570-017-1292-z

Zhao G-L, Hafrén J, Deiana L, Córdova A (2010) Heterogeneous "Organoclick" derivatization of polysaccharides: photochemical thiol-ene click modification of solid

cellulose. Macromol Rapid Commun 31(8):740–744. https://doi.org/10.1002/marc.200900764

Zhou L, He H, Li M-C, Huang S, Mei C, Wu Q (2018) Grafting polycaprolactone diol onto cellulose nanocrystals via click chemistry: enhancing thermal stability and hydrophobic property. Carbohydr Polym 189:331–341. https://doi.org/10.1016/j.carbpol.2018.02.039